Identification of Protein Targets of 4-Hydroxynonenal Using Click Chemistry for ex Vivo Biotinylation of Azido and Alkynyl Derivatives

Andrew Vila,[†,△] Keri A. Tallman,[‡,△] Aaron T. Jacobs,[†] Daniel C. Liebler,[‡,§] Ned A. Porter,[†,‡] and Lawrence J. Marnett*[,†,‡,§]

Departments of Biochemistry, Chemistry, and Pharmacology, Vanderbilt Institute of Chemical Biology, Center in Molecular Toxicology, Vanderbilt-Ingram Cancer Center, Vanderbilt University, Nashville, Tennessee 37232

Received September 25, 2007

Polyunsaturated fatty acids (PUFA) are primary targets of free radical damage during oxidative stress. Diffusible electrophilic α,β-unsaturated aldehydes, such as 4-hydroxynonenal (HNE), have been shown to modify proteins that mediate cell signaling (e.g., IKK and Keap1) and alter gene expression pathways responsible for inducing antioxidant genes, heat shock proteins, and the DNA damage response. To fully understand cellular responses to HNE, it is important to determine its protein targets in an unbiased fashion. This requires a strategy for detecting and isolating HNE-modified proteins regardless of the nature of the chemical linkage between HNE and its targets. Azido or alkynyl derivatives of HNE were synthesized and demonstrated to be equivalent to HNE in their ability to induce heme oxygenase induction and induce apoptosis in colon cancer (RKO) cells. Cells exposed to the tagged HNE derivatives were lysed and exposed to reagents to effect Staudinger ligation or copper-catalyzed Huisgen 1,3 dipolar cycloaddition reaction (click chemistry) to conjugate HNE-adducted proteins with biotin for subsequent affinity purification. Both strategies yielded efficient biotinylation of tagged HNE−protein conjugates, but click chemistry was found to be superior for the recovery of biotinylated proteins from streptavidin-coated beads. Biotinylated proteins were detected in lysates from RKO cell incubations with azido-HNE at concentrations as low as 1 μM. These proteins were affinity purified with streptavidin beads, and proteomic analysis was performed by linear ion trap mass spectrometry. Proteomic analysis revealed a dose-dependent increase in labeled proteins with increased sequence coverage at higher concentrations. Several proteins involved in stress signaling (heat shock proteins 70 and 90 and the 78-kDa glucose-regulated protein) were selectively adducted by azido- and alkynyl-HNE. The use of azido and alkynyl derivatives in conjunction with click chemistry appears to be a valuable approach for the identification of the protein targets of HNE.

Introduction

Reactive oxygen species generated under conditions of oxidative stress may initiate membrane lipid peroxidation (*1*). Among the many products generated from lipid oxidation is 4-hydroxynonenal (HNE[1]) (*2*). This α,β-unsaturated aldehyde covalently modifies DNA and protein resulting in genetic mutations and altered cell signaling, respectively (*3*). HNE modification of macromolecules may contribute to the progression of several diseases including atherosclerosis, ischemia-reperfusion injury, Parkinson's disease, and Alzheimer's disease (*4–8*).

Exposure of human colorectal cancer (RKO) cells to HNE elicits gene expression responses such as the induction of various antioxidant responsive, ER stress responsive, and heat shock responsive transcripts (*9*). Extensive protein damage from HNE treatment of RKO cells may account for the signaling responses observed. Several studies have demonstrated that protein modification by HNE or other electrophiles results in loss of protein function and disruption of cellular signaling. HNE modification of IκB kinase (IKK) (*10*), tubulin isoforms (*11*), and Keap1 (*12, 13*) leads to altered function in signaling pathways involved in NF-κB signaling, disruption of cytoskeletal function, and protection against oxidative injury, respectively. A comprehensive analysis of the proteins modified by HNE in vivo is necessary to understand the role of oxidative stress on cell signaling and disease pathology.

The modification of proteins by HNE predominantly occurs by Michael addition to nucleophilic amino acid residues His, Cys, and Lys with a minor amount of Schiff base adducts to Lys (*14*). The majority of previous studies identified HNE-adducted proteins using Anti-HNE antibodies. Anti-HNE antibodies directed against 4-HNE-sulfhydryl conjugates of keyhole limpet hemocyanin (KLH) generated in rabbit hosts (*15–18*) or

* To whom correspondence should be addressed. L. J. Marnett, Department of Biochemistry, Vanderbilt University School of Medicine, Nashville, TN 37232-0146. Tel: 615-343-7329. Fax: 615-343-7534. E-mail: larry.marnett@vanderbilt.edu.

† Department of Biochemistry.

‡ Department of Chemistry.

§ Department of Pharmacology.

△ These authors contributed equally to this work.

[1] Abbreviations: HNE, 4-hydroxy-2-nonenal; Az-HNE, azido-tagged HNE; Al-HNE, alkynyl-tagged HNE; Az-Biot, biotin-conjugated azide; Al-Biot, biotin-conjugated alkyne; BiotTPhPh, biotin-containing triphenyl phosphine; SA, streptavidin; HRP-SA, streptavidin-conjugated horseradish peroxidase; DMEM, Dulbecco's modified Eagle's medium; D-PBS, Dulbecco's phosphate buffered saline; TCEP, tris-(2-carboxyethyl)-phosphine-HCl; BHA, butylated hydroxyanisole; MS/MS, tandem MS; LC-MS/MS, liquid chromatography with electrospray ionization tandem MS; CHIPS, complete hierarchical integration of protein searches.

10.1021/tx700347w CCC: $40.75
Published on Web 01/31/2008

Scheme 1. Staudinger and Click Ligation Methods

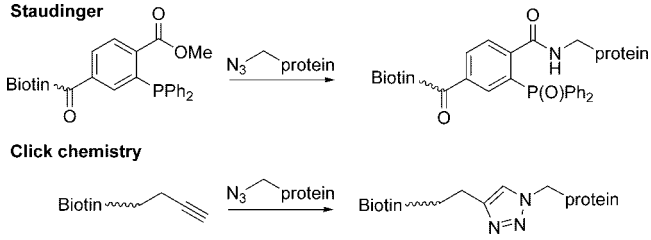

antibodies specific for HNE−Michael adducts (*10–13*) have been the most widely used for detecting HNE−protein adducts in cells and tissues. The first reported HNE−protein adducts were detected in a model of oxidative stress using carbon tetrachloride (CCl_4) treatment of isolated hepatocytes and rat liver (*18, 19*). The protein adducts were detected with the anti-HNE antibody specific for HNE−cysteine adducts. In a model of alcoholic liver disease, the same antibody was used to detect HNE-modified proteins on a Western blot of a 2D gel. The HNE-modified proteins were identified as Hsp72 (inducible form of Hsp70), Hsp90, and protein disulfide isomerase (PDI) by matrix-assisted laser desorption ionization time-of-flight mass spectrometry (MALDI-MS) and liquid chromatography with electrospray ionization (ESI) tandem MS (LC-MS/MS) (*15–17*). Additionally, the same antibody was used to identify the epithelial fatty acid binding protein (E-FABP) as a site of HNE adduction in rat retinal homogenates (*20*). The identifications of HNE-adducted protein in the above-mentioned studies are limited because only HNE adducts on cysteine were detectable with the antibody used.

Anti-HNE antibodies also show cross-reactivity with other lipid electrophiles. A rabbit polyclonal antibody detected HNE-modified proteins DRP-2, Hsp70, and α-enolase in a model of familial amyotrophic lateral sclerosis (*21*). The specificity of the antibody is for HNE− Michael adducts on His, Cys, and Lys of proteins; however, 4-hydroxy-2-decenal and 4-hydroxy-2-octenal can also be recognized (*22*). Another Michael adduct-specific anti-HNE antibody (*23*) recognizes the reduced form of the Lys-ONE Schiff base adduct, suggesting that this antibody is also not specific for HNE−protein adducts (*24*). For a comprehensive analysis of proteins modified by HNE, an unbiased approach for identifying all types of HNE−protein adducts is required. Also, a method for enriching HNE-adducted proteins over nonadducted proteins prior to LC-MS/MS analysis would enhance the overall identification of lower abundance protein adducts.

Recently, biotin hydrazide has been used as a reporter tag for proteins adducted by lipid oxidation products (*25*) and HNE (*26*) in vitro and in vivo. Biotin hydrazide is highly specific for free aldehyde groups on proteins (*27*) and several proteins involved in the cellular stress response, lipotoxicity, and insulin signaling were identified as being adducted by HNE. This method has an advantage over immunochemical approaches in that it recognizes HNE−protein adducts irrespective of the type of adduct formed, and the biotin tag provides enrichment of the labeled sample via biotin–avidin binding prior to LC-MS/MS analysis. Although HNE-adducted proteins were identified using this approach, oxidized proteins or proteins adducted by other lipid aldehyde products were also identified. Therefore, this method is not specific for proteins labeled with HNE.

Two recently developed methods for chemically tagging small molecules in cells offer promise for identifying the protein targets of reactive electrophiles such as HNE (Scheme 1). The first method was developed for selective labeling of membrane proteins containing glycoconjugates of azido-sugars with a biotin-containing triphenylphosphine (BiotTPhPh) using a modified Staudinger ligation (*28, 29*). The azido tag is stable in cells and provides a chemical handle for specifically enriching protein conjugates via biotin–avidin binding prior to LC-MS/MS analysis. The second method uses click chemistry, or the Huisgen 1,3-dipolar cycloaddition reaction, to conjugate azido or alkynyl probes to terminal alkyne or azide reporter tags (Biotin (*30*) or rhodamine (*31*)), respectively. Click chemistry has been used for activity-based protein profiling (ABPP) applications to identify serine esterase proteins in vivo (*31–33*). Click chemistry also provides a high fidelity reaction between protein targets in biological matrices and reporter groups similar to the Staudinger ligation (*34, 35*). Also, azido or alkynyl probes can be used for labeling cellular constituents followed by coupling to alkynyl or azido reporter tags, respectively. Proteins tagged with biotin from either of the above-mentioned methods can be enriched through biotin–avidin binding prior to LC-MS/MS analysis.

In the present study, we applied both the modified Staudinger ligation and click chemistry approaches to label proteins in RKO cells with HNE (**1**). Azido-tagged HNE (Az-HNE, **2**) was used to label proteins in intact RKO cells followed by conjugation to BiotTPhPh (**4**) using the modified Staudinger ligation. For click chemistry, both Az-HNE and alkynyl-tagged HNE (Al-HNE, **3**) were used to label proteins in intact cells followed by conjugation with the appropriate biotin conjugated alkyne (Al-Biot, **5**) or azido (Az-Biot, **6**), respectively. Biotin-conjugated proteins were then enriched using streptavidin (SA) beads prior to LC-MS/MS analysis. The results demonstrate that biotin labeling of Az-HNE-adducted proteins via the modified Staudinger ligation is efficient, but purification of biotin-labeled proteins from background proteins using SA beads is difficult. The use of click chemistry resulted in specific biotin labeling of Az-HNE- and Al-HNE-adducted proteins and selective SA bead purification of biotin-tagged proteins. Subsequent proteomic analysis of these proteins revealed a broad spectrum of targets for HNE.

Materials and Methods

Materials. Streptavidin conjugated to horseradish peroxidase (HRP-SA), bovine serum albumin (BSA), sodium cyanoborohydride ($NaCNBH_3$), protease inhibitor cocktail (PIC) for mammalian cell culture, dithiothreitol (DTT), and sodium ascorbate (Asc) were purchased from Sigma-Aldrich (St. Louis, MO). Streptavidin coupled to 6% cross-linked sepharose beads was from GE Healthcare (Picataway, NJ). Laemmli buffer, and silver staining kit were from Biorad (Hercules, CA). Anhydrous $CuSO_4$ was from Fisher (Pittsburgh, PA). Gradient gels (4–20% polyacrylamide) were from Invitrogen (Carlsbad, CA). Handee mini spin filters, M-Per cell lysis buffer, West Pico ECL kit, and tris-(2-carboxyethyl)-phosphine•HCl (TCEP) were purchased from Pierce (Rockford, Il). Iodoacetamide was from Aldrich (Milwaukee, WI). Modified trypsin, mass spectrometry grade, was from Promega (Madison, WI). Western blotting was accomplished with Kodak Biomax light film (Sigma) with ECL detection in an Electrophoresis Systems Autoradiography Cassette (FisherBiotech; Wembley, WA).

General Methods. ^1H and ^{13}C NMR spectra were collected on a 300 MHz NMR spectrometer. All reactions were carried out under an atmosphere of argon. $CH_2Cl_2$was dried using a solvent purification system. Commercial anhydrous DMSO, DMF, and CH_3CN were used as received. Purification by column chromatography was carried out on silica gel, and TLC plates were visualized with phosphomolybdic acid. HNE (**1**) and its analogues (**2** and **3**) were synthesized following the same procedures; representative procedures for HNE are presented as well as the characterization for all

compounds. 6-Heptynal (*36*), **7** (*37*), **12** (*38*), and 6-azidohexanoic acid (*39*) were synthesized by literature procedures.

Synthesis of 7-Azidoheptanal. NaN_3 (2.3 g, 0.035 mol) was added to a solution of 7-bromoheptanol (3.6 mL, 0.023 mol) in DMSO (75 mL). After stirring overnight, the reaction mixture was diluted with H_2O and extracted with ether. The organics were washed with brine and dried over $MgSO_4$. The product was isolated as a pale yellow liquid (3.9 g, 100%) and used without purification. ^{1}H NMR ($CDCl_3$) δ 3.62 (t, 2H, J = 6.6 Hz), 3.22 (t, 2H, J = 6.9 Hz), 1.54 (m, 5H), 1.36 (m, 6H); ^{13}C NMR ($CDCl_3$) δ 62.8, 51.4, 32.5, 28.9, 28.7, 26.6, 25.6. Oxalyl chloride (2.7 mL, 0.030 mol) was added to a solution of DMSO (4.1 mL, 0.058 mol) in CH_2Cl_2 (100 mL) at −78 °C. After 30 min, 7-azidoheptanol (3.9 g, 0.023 mol) was added and the reaction mixture stirred for 30 min, followed by the addition of Et_3N (16 mL, 0.11 mol). After stirring overnight, the reaction mixture was diluted with H_2O and extracted with ether. The organics were washed with 10% HCl, saturated $NaHCO_3$, and brine, and dried over $MgSO_4$. Purification by column chromatography (10% EtOAc/hexanes) afforded the product as a pale yellow liquid (2.9 g, 81%). Characterization of 7-azidoheptanal was consistent with the literature (*40*). ^{1}H NMR ($CDCl_3$) δ 9.73 (t, 1H, J = 1.5 Hz), 3.23 (t, 2H, J = 6.9 Hz), 2.41 (dt, 2H, J = 1.8, 7.2 Hz), 1.58 (m, 4H), 1.34 (m, 4H); ^{13}C NMR ($CDCl_3$) δ 202.5, 51.3, 43.7, 28.6, 26.4, 21.8.

Synthesis of (*E*)-Ethyl 4-hydroxy-2-nonenoate (8). Heptaldehyde (2.9 mL, 0.021 mol), 6-heptynal, or 7-azidoheptanal and piperidine (2.8 mL, 0.028 mol) were added to a solution of **7** (3.3 g, 0.014 mol) in CH_3CN (70 mL). After stirring overnight, the reaction mixture was diluted with saturated NH_4Cl and extracted with CH_2Cl_2. The organic layer was dried over $MgSO_4$. The product was purified by column chromatography (20% EtOAc/hexanes) and isolated as a yellow liquid (2.6 g) in 91% yield.

8a (R = CH_2CH_3): ^{1}H NMR ($CDCl_3$) δ 6.91 (dd, 1H, J = 4.8, 15.6 Hz), 6.00 (dd, 1H, J = 1.5, 15.6 Hz), 4.27 (m, 1H), 4.17 (q, 2H, J = 7.2 Hz), 1.88 (d, 1H, J = 4.8 Hz), 1.55 (m, 2H), 1.30 (m, 6H), 1.26 (t, 3H, J = 7.2 Hz), 0.86 (m, 3H); ^{13}C NMR ($CDCl_3$) δ 166.6, 150.2, 120.1, 71.1, 60.4, 36.6, 31.6, 24.8, 22.5, 14.2, 14.0; HRMS (MALDI) calculated, 201.1491 (M + H); observed, 201.1493.

8b (R = C≡CH): ^{1}H NMR ($CDCl_3$) δ 6.91 (dd, 1H, J = 4.8, 15.6 Hz), 6.00 (dd, 1H, J = 1.5, 15.6 Hz), 4.31 (m, 1H), 4.16 (q, 2H, J = 7.2 Hz), 2.21 (m, 2H), 2.07 (d, 1H, J = 4.8 Hz), 1.94 (t, 1H, J = 2.7 Hz), 1.67 (m, 4H), 1.26 (t, 3H, J = 7.2 Hz); ^{13}C NMR ($CDCl_3$) δ 166.5, 149.8, 120.4, 83.8, 70.5, 68.8, 60.5, 35.4, 24.0, 18.2, 14.2; HRMS (MALDI) calculated, 197.1178 (M + H); observed, 197.1181.

8c (R = $(CH_2)_2N_3$): ^{1}H NMR ($CDCl_3$) δ 6.90 (dd, 1H, J = 5.1, 15.6 Hz), 5.99 (dd, 1H, J = 1.5, 15.6 Hz), 4.28 (m, 1H), 4.16 (q, 2H, J = 7.2 Hz), 3.23 (t, 2H, J = 6.6 Hz), 2.00 (d, 1H, J = 3.6 Hz), 1.57 (m, 4H), 1.36 (m, 4H), 1.26 (t, 3H, J = 7.2 Hz); ^{13}C NMR ($CDCl_3$) δ 166.5, 150.0, 120.2, 70.9, 60.5, 51.3, 36.3, 28.7, 26.5, 24.7, 14.2; HRMS (MALDI) calculated, 248.1586 (M + Li); observed, 248.1578.

Synthesis of (*E*)-Ethyl 4-(*tert*-Butyldimethylsilyloxy)-2-nonenoate (9). TBDMSCl (2.5 g, 0.017 mol) and imidazole (2.4 g, 0.035 mol) were added to a solution of **8** (2.6 g, 0.013 mol) in DMF (30 mL). After stirring overnight, the reaction mixture was diluted with H_2O and extracted with ether. The organic layer was washed with brine and dried over $MgSO_4$. The product (3.2 g, 78%) was isolated as a colorless liquid after column chromatography (10% EtOAc/hexanes).

9a (R = CH_2CH_3): ^{1}H NMR ($CDCl_3$) δ 6.90 (dd, 1H, J = 4.8, 15.6 Hz), 5.93 (dd, 1H, J = 1.5, 15.3 Hz), 4.26 (m, 1H), 4.17 (dq, 2H, J = 1.5, 7.2 Hz), 1.50 (m, 2H), 1.29–1.25 (m, 6H), 1.27 (t, 3H, J = 6.9 Hz), 0.88 (s, 9H), 0.85 (t, 3H, J = 6.9 Hz), 0.03 (s, 3H), 0.01 (s, 3H); ^{13}C NMR ($CDCl_3$) δ 166.8, 151.2, 119.6, 71.6, 60.3, 37.3, 31.8, 25.8, 24.5, 22.5, 18.2, 14.3, 14.0, −4.6, −4.9; HRMS (MALDI) calculated, 315.2355 (M + H); observed, 315.2353.

9b (R = C≡CH): ^{1}H NMR ($CDCl_3$) δ 6.88 (dd, 1H, J = 4.8, 15.6 Hz), 5.95 (dd, 1H, J = 1.8, 15.6 Hz), 4.33 (m, 1H), 4.17 (dq, 2H, J = 1.5, 7.2 Hz), 2.18 (dt, 2H, J = 2.7, 6.9 Hz), 1.92 (t, 1H, J = 2.7 Hz), 1.60 (m, 4H), 1.27 (t, 3H, J = 7.2 Hz), 0.89 (s, 9H), 0.04 (s, 3H), 0.01 (s, 3H); ^{13}C NMR ($CDCl_3$) δ 166.6, 150.5, 120.1, 84.0, 71.0, 68.6, 60.3, 36.1, 25.8, 23.5, 18.4, 18.2, 14.2, −4.6, −5.0; HRMS (MALDI) calculated, 311.2042 (M + H); observed, 311.2046.

9c (R = $(CH_2)_2N_3$): ^{1}H NMR ($CDCl_3$) δ 6.88 (dd, 1H, J = 4.8, 15.6 Hz), 5.94 (dd, 1H, J = 1.5, 15.6 Hz), 4.28 (m, 1H), 4.17 (dq, 2H, J = 3.9, 7.2 Hz), 3.23 (t, 2H, J = 6.9 Hz), 1.54 (m, 4H), 1.34 (m, 4H), 1.27 (t, 3H, J = 7.2 Hz), 0.88 (s, 9H), 0.03 (s, 3H), 0.01 (s, 3H); ^{13}C NMR ($CDCl_3$) δ 166.7, 150.8, 119.9, 71.3, 60.3, 51.3, 37.1, 28.7, 26.7, 25.8, 24.2, 18.2, 14.2, −4.6, −5.0.

Synthesis of (*E*)-4-(*tert*-Butyldimethylsilyloxy)-2-nonen-1-ol (10). DIBAL-H (20 mL of 1.4 M/toluene, 0.028 mol) was added to a solution of **9** (3.2 g, 0.010 mol) in CH_2Cl_2 (50 mL) at 0 °C. After 30 min, the reaction mixture was quenched with 10% HCl and extracted with CH_2Cl_2. The organics were dried over $MgSO_4$ and purified by column chromatography (10% EtOAc/hexanes). The product (2.6 g) was isolated as a colorless liquid in 93% yield.

10a (R = CH_2CH_3): ^{1}H NMR ($CDCl_3$) δ 5.69 (m, 2H), 4.09 (m, 3H), 1.45 (m, 2H), 1.25 (m, 7H), 0.87 (s, 9H), 0.86 (t, 3H, J = 6.9 Hz), 0.03 (s, 3H), 0.00 (s, 3H); ^{13}C NMR ($CDCl_3$) δ 135.5, 128.1, 72.7, 63.3, 38.2, 31.8, 25.9, 24.9, 22.6, 18.2, 14.1, −4.3, −4.8; HRMS (MALDI) calculated, 273.2250 (M + H); observed, 273.2248.

10b (R = C≡CH): ^{1}H NMR ($CDCl_3$) δ 5.69 (m, 2H), 4.12 (m, 3H), 2.16 (m, 2H), 1.91 (t, 1H, J = 2.7 Hz), 1.53 (m, 5H), 0.86 (s, 9H), 0.02 (s, 3H), 0.00 (s, 3H); ^{13}C NMR ($CDCl_3$) δ 134.9, 128.6, 84.4, 72.2, 68.4, 63.1, 37.1, 25.9, 24.1, 18.4, 18.2, −4.3, −4.8; HRMS (MALDI) calculated, 269.1937 (M + H); observed, 269.1940.

10c (R = $(CH_2)_2N_3$): ^{1}H NMR ($CDCl_3$) δ 5.67 (m, 2H), 4.11 (m, 3H), 3.23 (t, 2H, J = 6.9 Hz), 1.56 (m, 2H), 1.47 (m, 2H), 1.32 (m, 5H), 0.87 (s, 9H), 0.02 (s, 3H), 0.00 (s, 3H); ^{13}C NMR ($CDCl_3$) δ 135.1, 128.4, 72.5, 63.2, 51.4, 38.0, 28.8, 26.7, 25.9, 24.6, 18.2, −4.3, −4.8; HRMS (MALDI) calculated, 320.2346 (M + Li); observed, 320.2348.

Synthesis of (*E*)-4-(*tert*-Butyldimethylsilyloxy)-2-nonenal (11). Oxalyl chloride (0.65 mL, 7.3 mmol) was added to a solution of DMSO (1.0 mL, 14 mmol) in CH_2Cl_2 (28 mL) at −78 °C. After 20 min, a solution of **10** (1.5 g, 5.6 mmol) in CH_2Cl_2 (10 mL) was added. After 30 min, Et_3N (3.9 mL, 28 mmol) was added and the reaction mixture allowed to warm to room temperature. After 3 h, the reaction mixture was diluted with H_2O and extracted with ether. The organic layer was washed with 10% HCl, saturated $NaHCO_3$, and brine, and dried over $MgSO_4$. Purification by column chromatography (10% EtOAc/hexanes) afforded the product (1.2 g, 82%) as a colorless liquid.

11a (R = CH_2CH_3): ^{1}H NMR ($CDCl_3$) δ 9.54 (d, 1H, J = 8.1 Hz), 6.77 (dd, 1H, J = 4.5, 15.3 Hz), 6.23 (ddd, 1H, J = 1.5, 7.8, 15.3 Hz), 4.38 (m, 1H), 1.54 (m, 2H), 1.28 (m, 6H), 0.88 (s, 9H), 0.85 (t, 3H, J = 6.9 Hz), 0.04 (s, 3H), 0.00 (s, 3H); ^{13}C NMR ($CDCl_3$) δ 193.7, 160.3, 130.6, 71.6, 37.1, 31.7, 25.8, 24.5, 22.5, 18.1, 14.0, −4.7, −4.9; HRMS (MALDI) calculated, 271.2093 (M + H); observed, 271.2097.

11b (R = C≡CH): ^{1}H NMR ($CDCl_3$) δ 9.54 (d, 1H, J = 8.1 Hz), 6.76 (dd, 1H, J = 4.5, 15.6 Hz), 6.24 (ddd, 1H, J = 1.5, 8.1, 15.6 Hz), 4.44 (m, 1H), 2.18 (dt, 2H, J = 2.7, 6.9 Hz), 1.93 (t, 1H, J = 2.7 Hz), 1.69 (m, 2H), 1.56 (m, 2H), 0.88 (s, 9H), 0.04 (s, 3H), 0.00 (s, 3H); ^{13}C NMR ($CDCl_3$) δ 193.5, 159.6, 130.9, 83.8, 71.1, 68.8, 35.8, 25.7, 23.5, 18.3, 18.1, −4.7, −5.0; HRMS (MALDI) calculated, 267.1780 (M + H); observed, 267.1777.

11c (R = $(CH_2)_2N_3$): ^{1}H NMR ($CDCl_3$) δ 9.55 (d, 1H, J = 7.8 Hz), 6.76 (dd, 1H, J = 4.8, 15.6 Hz), 6.24 (ddd, 1H, J = 1.5, 7.8, 15.3 Hz), 4.41 (m, 1H), 3.24 (t, 2H, J = 6.9 Hz), 1.57 (m, 4H), 1.36 (m, 4H), 0.88 (s, 9H), 0.04 (s, 3H), 0.01 (s, 3H); ^{13}C NMR ($CDCl_3$) δ 193.6, 159.9, 130.8, 71.4, 51.3, 36.9, 28.7, 26.7, 25.7, 24.3, 18.1, −4.7, −4.9; HRMS (MALDI) calculated, 318.2189 (M + Li); observed, 318.2199.

Synthesis of (*E*)-4-Hydroxy-2-nonenal (1). Aqueous HF (0.5 mL) was added to a solution of **11** (0.55 g, 2.0 mmol) in CH_3CN

(10 mL). After 1 h, the reaction mixture was diluted with H_2O and extracted with CH_2Cl_2. The organic layer was dried over $MgSO_4$. The product (0.3 g) was isolated as a colorless liquid after column chromatography (20% EtOAc/hexanes) in 88% yield.

1 (R = CH_2CH_3): ^{1}H NMR ($CDCl_3$) δ 9.53 (d, 1H, J = 7.8 Hz), 6.80 (dd, 1H, J = 4.8, 15.9 Hz), 6.27 (ddd, 1H, J = 1.5, 8.1, 15.6 Hz), 4.39 (m, 1H), 2.35 (d, 1H, J = 4.5 Hz), 1.59 (m, 2H), 1.34 (m, 6H), 0.86 (t, 3H, J = 6.6 Hz); ^{13}C NMR ($CDCl_3$) δ 193.8, 159.4, 130.5, 71.0, 36.4, 31.5, 24.8, 22.5, 13.9; HRMS (MALDI) calculated, 163.1310 (M + Li); observed, 163.1316.

2 (R = C≡CH): ^{1}H NMR ($CDCl_3$) δ 9.54 (d, 1H, J = 7.8 Hz), 6.81 (dd, 1H, J = 4.5, 15.6 Hz), 6.29 (ddd, 1H, J = 1.8, 8.1, 15.9 Hz), 4.46 (m, 1H), 2.35 (d, 1H, J = 4.5 Hz), 2.23 (dt, 2H, J = 2.7, 6.6 Hz), 1.95 (t, 1H, J = 2.7 Hz), 1.72 (m, 4H); ^{13}C NMR ($CDCl_3$) δ 193.6, 158.8, 130.7, 83.7, 70.4, 69.0, 35.1, 23.9, 18.1; HRMS (MALDI) calculated, 159.0997 (M + Li); observed, 159.0989.

3 (R = $(CH_2)_2N_3$): ^{1}H NMR ($CDCl_3$) δ 9.53 (d, 1H, J = 7.8 Hz), 6.80 (dd, 1H, J = 4.8, 15.6 Hz), 6.27 (ddd, 1H, J = 1.5, 7.8, 15.6 Hz), 4.40 (m, 1H), 3.24 (t, 2H, J = 6.9 Hz), 2.41 (br s, 1H), 1.58 (m, 4H), 1.42 (m, 4H); ^{13}C NMR ($CDCl_3$) δ 193.7, 159.1, 130.6, 70.8, 51.2, 36.1, 28.6, 26.5, 24.7; HRMS (MALDI) calculated, 204.1324 (M + Li); observed, 204.1333.

Synthesis of Biotin Alkyne (5). Oxalyl chloride (2.4 mL, 0.027 mol) was added to a solution of 5-hexynoic acid (2.0 mL, 0.018 mol) and DMF (0.30 mL, 0.0039 mol) in benzene (18 mL). After 2 h, the reaction mixture was concentrated. A solution of the acid chloride in DMF (3.6 mL of 1.8 M, 6.5 mmol) was added to a solution of **12** (2.0 g, 5.3 mmol) and Et_3N (1.1 mL, 7.9 mmol) in DMF (25 mL). After stirring overnight, the reaction mixture was concentrated under high vacuum and purified by column chromatography (10% MeOH/CH_2Cl_2). A solution of the product in MeOH was passed through basic Dowex to remove triethylammonium salts and isolated as an off-white powder (1.4 g, 57%). ^{1}H NMR (MeOH-d_4) δ 4.49 (dd, 1H, J = 4.8, 7.8 Hz), 4.30 (dd, 1H, J = 4.5, 7.8 Hz), 3.61 (s, 4H), 3.54 (t, 4H, J = 5.7 Hz), 3.36 (t, 4H, J = 5.4 Hz), 3.20 (m, 1H), 2.92 (dd, 1H, J = 5.1, 12.9 Hz), 2.70 (d, 1H, J = 12.9 Hz), 2.31 (t, 2H, J = 7.2 Hz), 2.21 (m, 5H), 1.79 (pentet, 2H, J = 7.5 Hz), 1.64 (m, 4H), 1.43 (m, 2H); ^{13}C NMR (MeOH-d_4) δ 176.1, 175.4, 166.0, 84.2, 71.2, 70.6, 70.5, 63.3, 61.6, 57.0, 54.8, 41.1, 40.2, 36.7, 35.8, 29.7, 29.5, 26.8, 25.9, 18.6; HRMS (MALDI) calculated, 469.2485 (M + H); observed, 469.2488.

Synthesis of Biotin Azide (6). Biotin reagent **6** was synthesized starting from 6-azidohexanoic acid as described above and isolated as an off-white powder (1.4 g, 53%). ^{1}H NMR (MeOH-d_4) δ 4.49 (dd, 1H, J = 4.8, 7.8 Hz), 4.30 (dd, 1H, J = 4.2, 7.8 Hz), 3.61 (s, 4H), 3.54 (t, 4H, J = 5.7 Hz), 3.35 (t, 4H, J = 5.4 Hz), 3.29 (t, 2H, J = 6.9 Hz), 3.20 (m, 1H), 2.92 (dd, 1H, J = 5.1, 12.9 Hz), 2.70 (d, 1H, J = 12.9 Hz), 2.21 (t, 4H, J = 7.2 Hz), 1.65 (m, 8H), 1.42 (m, 4H); ^{13}C NMR (MeOH-d_4) δ 176.10, 176.05, 166.1, 71.3, 70.6, 63.3, 61.6, 57.0, 52.3, 41.1, 40.3, 36.8, 36.7, 29.8, 29.6, 29.5, 27.4, 26.8, 26.5; HRMS (MALDI) calculated, 514.2812 (M + H); observed, 514.2817.

Peptide Adduction. Stock solutions of peptides (1 mM) were prepared in phosphate buffer (50 mM, pH 7.4) and stock solutions of HNE and analogues (51 mM) were prepared in DMSO. Initial experiments were carried out with peptide (90 μL, 0.9 mM) and HNE (10 μL, 5 mM) to identify the peptide adducts. For experiments in which the reactivity of the analogues was compared to HNE, samples were prepared with peptide (70 μL, 0.7 mM) and an equimolar mixture of each HNE compound (10 μL of each HNE, 5 mM each). In all experiments, the samples were incubated at 37 °C, typically for 1 h. The reaction mixture was subsequently reduced with $NaBH_4$ (100 mM) then neutralized with 1 M HCl (10 μL) for LC-MS analysis. The reaction mixture was analyzed on a Discovery C18 column using a mobile phase consisting of A, 0.05% TFA in H_2O and B, 0.05% TFA in CH_3CN. The unreacted peptide and adducts were eluted with a gradient of 15% to 35% B over 20 min, then to 90% B over 10 min, and back to 15% B over 5 min.

Biological Activity of HNE, Az-, and Al-HNE. For cell viability assays, RKO cells were seeded in 96-well plates at a density of 7,500 cells per well. After adhering overnight, cells were treated with HNE, Az-, or Al-HNE at concentrations ranging from 1 to 80 μM in DMEM containing 10% fetal bovine serum (FBS) with vehicle control (DMSO 0.5%, v/v) run alongside. Following 48 h of incubation, media was aspirated, washed once in Dulbecco's phosphate buffered saline (D-PBS) and replaced with a solution of 1 μM calcein-AM (Molecular Probes) in D-PBS. After 30 min, the fluorescence was measured using a SpectrasMax multiwell plate reader (Molecular Devices) using an excitation of 494 nm, and an emission of 517 nm.

Induction of Heme-oxygenase-1 (HO-1) expression was done by incubating RKO cells with 5 and 25 μM HNE, Az-, or Al-HNE for 8 h. Cells were lysed using M-Per buffer with 1% PIC, and HO-1 expression was monitored by Western blotting using an anti HO-1 antibody from BD Biosciences.

Click Chemistry of Peptide Adducts. Stock solutions of **5** (100 mM), **6** (100 mM), and ligand (100 mM) were prepared in DMSO. Stock solutions of sodium ascorbate (500 mM) and $CuSO_4$ (500 mM) were prepared in H_2O. An aliquot (40 uL) of the peptide adduction mixture described above was diluted with H_2O (260 uL) and CH_3CN (100 uL) so that the HNE analogue concentration was 0.5 mM. The use of CH_3CN as a cosolvent was necessary to ensure complete dissolution of all reagents. The appropriate biotin reagent (**5** or **6**, 20 μL, 5 mM), ascorbate (20 μL, 25 mM), ligand (20 μL, 5 mM), and $CuSO_4$ (20 μL, 25 mM) were added to the peptide adduct, vortexed, and allowed to react at room temperature, typically for 1 h. The samples were analyzed by LC-MS as described above.

Adduction of Biotin to HNE-Modified Proteins in Intact RKO Cells Using the Modified Staudinger Ligation or Click Chemistry. RKO cells were seeded in 10 cm plates at 2.0 × 10^6 cells/plate in DMEM with FBS. The following morning, cells were washed with 5 mL of D-PBS (2×) followed by the addition of Az-HNE or Al-HNE in 5 mL of DMEM lacking FBS with DMSO (1% v/v) or vehicle control (DMSO only) for 1 h at 37 °C. Cells were then washed twice with D-PBS, scraped into 5 mL of PBS, and collected after centrifugation (1,000 rpms, 5 min, 4 °C). For the modified Staudinger ligation (Az-HNE concentrations 50, 100, and 150 μM), cells were scraped washed again by centrifugation, and lysed in M-Per lysis buffer containing 1% PIC for 20 min on ice followed by sonication (10 pulses for 10 s, 35% power, 4 °C). Freshly prepared $NaCNBH_3$ (0.5 M in D-PBS) was added to the cell lysates and incubated for 1 h to reduce Schiff base adducts and reversible Michael adducts (*41*). BiotTPhPh (200 μM) was added for 1 h, and the sample was quenched by boiling in laemmli buffer with 5% β-mercaptoethanol, followed by Western blot analysis to assess the level of biotin-tagging.

Click chemistry was performed with cellular lysates containing 1.0 mg/mL of protein with 0.6 mM of the appropriate biotin reagent (Al-Biot or Az-Biot) (0.6 mM), TCEP (6 mM), ligand (**13**, 0.75 mM), and $CuSO_4$ (6 mM). RKO cells treated with Az-HNE (1, 5, 10, 25, or 50 μM) or vehicle control were lysed as described above. For assessing the time-dependence of Al-Biot conjugation with Az-HNE, adducted proteins aliquots were removed from the incubation at 0, 1.5, 3, and 6 h and added to an equal volume of laemmli buffer containing 5% β-mercaptoethanol, 10 mM EDTA, and 100 μM BHA to quench the reaction. Samples were prepared for SA beads as described below. RKO cells treated with Al-HNE (5, 10, or 50 μM) were lysed with 100 mM HEPES at pH 7.5, 150 mM NaCl, 0.1 mM EDTA, and 1% Igepal with 1% PIC, processed as described above, and treated with Az-Biot for 2 h prior to SA bead purification.

Purification of Biotin-Tagged Proteins from the Modified Staudinger Ligation and Click Chemistry with Streptavidin Beads. Purification of biotin-tagged proteins from the modified Staudinger ligation was done with 30 μL of cell lysates (~7.5 μg of total protein) and 45 μL of SA beads (1:1 slurry in 0.1 M ammonium bicarbonate) in Handee mini-spin columns with end-over-end rotation for 1 h. After 1 h, the beads were pelleted at 6,500*g* for 5 min, and the supernatant was collected as the breakthrough fraction (proteins that are not retained by streptavidin beads). The beads were washed successively with ammonium bicarbonate, 1 M NaCl with 1% Igepal, ammonium bicarbonate,

and distilled H_2O. The first elution of biotin-tagged proteins was accomplished with 70% CH_3CN and 5% formic acid (FA). Another wash with distilled H_2O was done, and an equal volume of laemmli buffer with (5% β-mercaptoethanol) was added to the SA beads and boiled for 10 min for the second elution. Both Western blot and silver stain analysis were carried out to determine where biotin-tagged proteins and total proteins were eluting, respectively.

Biotin-tagged proteins from click chemistry reactions were centrifuged (5,000*g*, 5 min, 4 °C) and recovered in the pellet, washed in ice-cold methanol, and then resuspended by sonication (5 s). Supernatant solutions contained undetectable levels of protein (BCA assay) and biotin-conjugated protein (Western blotting) (data not shown). The samples were then rotated end-over-end at 4 °C for 10 min and centrifuged, and the supernatant was removed. Following another methanol wash, protein samples were solubilized in 0.1 M ammonium bicarbonate containing 0.2% SDS. Cell lysates treated with control, 5, 10, and 50 μM for Az-HNE were incubated with streptavidin-conjugated sepharose (SA) beads overnight in Handee mini-spin columns on a shaker at 60 rpms. Each sample contained a total of 150 μg of protein (0.5 mg/mL) with 75 μL of 1:1 slurry of SA beads in ammonium bicarbonate. Lysates from Al-HNE-treated (5, 10, and 50 μM) RKO cells contained 2 mg of protein (1.0 mg/mL) and were incubated with a total of 1 mL of SA beads in 1.5 mL tubes for 2 h. Also, click chemistry reactions with Az-HNE-adducted proteins from RKO cells were done using 2 mg of cell lysate for comparison with Al-HNE. The 1.5 mL tubes were centrifuged (6,500*g*, 5 min), and the breakthrough fraction was collected. More stringent wash steps were used in the experiments with 2 mg of cellular lysate. The beads were washed successively with 1% SDS, 4 M urea, 1 M NaCl, ammonium bicarbonate, and distilled water. The beads were incubated for 30 min with 1% SDS and 4 M urea, and for 10 min with 1 M NaCl with end-over-end rotation prior to pelleting the beads. Biotin-tagged proteins were eluted as described above.

Proteomic Analysis of Captured Proteins. Biotin-tagged proteins from Coomassie stained gels were subjected to in-gel digestion, followed by peptide extraction, and proteomic analysis by LC-MS/MS using an established procedure (*42*). Biotin-tagged proteins purified with SA beads were run on a gradient gel (4–20% acrylamide) and visualized with colloidal Coomassie blue (Invitrogen). Visible bands were excised by cutting the entire molecular weight range into 10 fractions with industrial razor blades (VWR), which were further sliced into ~1 mm cubes, and placed into a 1.5 mL eppendorf tube. The cubes were washed once with 100 μL of ammonium bicarbonate and centrifuged, and another 100 μL of ammonium bicarbonate was added. DTT was added to a final concentration of 3 mM, and the cubes were incubated for 15 min at 50 °C followed by incubation with iodoacetamide (6.25 mM final conc) for 15 min. The samples were then equilibrated with 50:50 CH_3CN/ammonium bicarbonate for 15 min to remove the blue stain. The gel cubes were then dehydrated with 100% CH_3CN followed by desiccation in a vacuum centrifuge. The dehydrated gel slices were reswelled with 25 μL of 0.01 μg/μL modified trypsin in 25 mM ammonium bicarbonate and incubated overnight at 37 °C. Peptides were extracted with 50 μL of 60% CH_3CN, 1% FA (2×), evaporated in vacuo, resuspended in distilled water with 1% FA, and then desalted using Zip-Tips (Millipore C_{18}, P10). The peptide eluant from the Zip-Tips was evaporated, and 50 μL of distilled water with 0.1% FA was added followed by LC-MS/MS analysis.

The samples were analyzed on a Thermo LTQ linear ion trap instrument equipped with a Thermo microelectrospray source, and a Thermo Surveyor pump and autosampler. LC-MS/MS analyses were done by reverse phase chromatography on an 11 cm fused silica capillary column (100 μm i.d.) packed with Jupiter C-18 (5 μm) resin set to a flow rate of 700 nL/min. The mobile phase consisted of 0.1% formic acid in either HPLC grade H_2O (A) or CH_3CN (B), and sample runs were 95 min in length. The peptide samples were injected onto the column at 98% A, which was held for 15 min, followed by a linear gradient from 98% A to 75% A for 50 min. A linear gradient to 10% A at 65 min was done followed by isocratic conditions of 10% A to 74 min followed by re-equilibration to 98% A. MS/MS spectra were acquired using one data-dependent scan from the most intense precursor ion in the full scan mode. The MS/MS spectra were matched to human database sequences with TurboSequest. S-carbomethylation of Cys (+57 amu) and oxidation of Met (+16 amu) were specified as dynamic modifications. Sequest output files were filtered with the software database system CHIPS (Complete Hierarchical Integration of Protein Searches). Sequence-spectrum assignments were accepted on the basis of the following filtering criteria: (1) all peptide sequence assignments were required to result from fully tryptic cleavages, (2) singly, doubly, and triply charged ions were accepted if their XCorr scores were greater than 2, 2.5, and 3, respectively, and (3) all putative matches were confirmed by visual inspection of the spectra. Identifications were accepted only for proteins with 3 unique peptide identifications matching high quality MS/MS spectra. The lists of proteins from vehicle control, 5, 10, and 50 μM Az- and Al-HNE treated cells were compared in CHIPS.

Scheme 2. Synthesis of HNE and Analogues

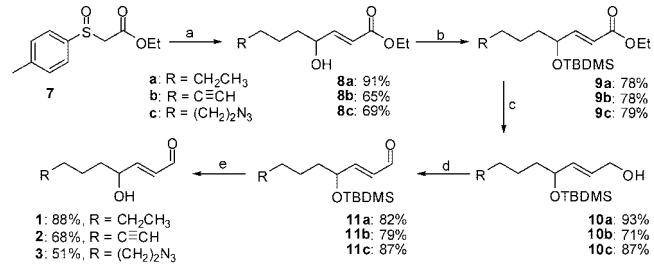

Reagents: a) aldehyde, piperidine, CH_3CN; b) TBDMSCl, imidazole, DMF; c) DIBAL-H, CH_2Cl_2, 0 °C; d) Swern oxidation; e) HF_{aq}, CH_3CN.

SDS−PAGE and Western Blotting with ECL Detection. Tris-glycine polyacrylamide gels (4–20%) were used for separating proteins. Samples in laemmli sample buffer with 5% β-mercaptoethanol were run on the gels for 1 h at 150 V. The silver stain plus kit (Biorad) was used to fix and stain gels for the visualization of total protein. Visualization of biotin-tagged protein was done by Western blot analysis. Proteins separated on gradient gels were transferred to a 0.2 μm nitrocellulose membrane for 1 h in SDS−PAGE transfer buffer (1× running buffer with 20% MeOH) at 100 V. The membranes were blocked with PBS with Tween20 (0.1% v/v) (PBS-T) for 1 h and then blotted with HRP-SA (100 ng/mL) for an additional hour. The membranes were then washed in PBS-T, and biotin-tagged proteins recognized by HRP-SA were detected on BioMax light film using the SuperSignal West Pico Chemiluminescent Substrate.

Results

Synthesis of HNE Analogues and Biotin Tags. HNE and its analogues were synthesized in a similar manner (Scheme 2), modified from a previously reported procedure (*37*). Sulfinate **7** was coupled with the appropriate aldehyde to yield the α,β-unsaturated esters (**8**) in good yields. Subsequent protection of the alcohol as the silyl ether was necessary to enable facile reduction of the ester to the alcohol (**10**). The ester was selectively reduced to the alcohol using DIBAL-H, whereas $LiAlH_4$ also reduced the olefin. Alcohol **10** was oxidized to the aldehyde (**11**) under Swern conditions and finally deprotected to yield HNE and its analogues (**1**–**3**). Several common silyl deprotection strategies were explored, such as TBAF and pyridine-HF, but we found significant decomposition of the product under these conditions. Optimum yields were obtained when the mild HF conditions were used.

BiotTPhPh was synthesized according to previous procedures (*28*). The biotin reagents for click chemistry were designed to contain either an azide or alkyne functionality for coupling to **2** and **3**, respectively, under click conditions. In addition, the

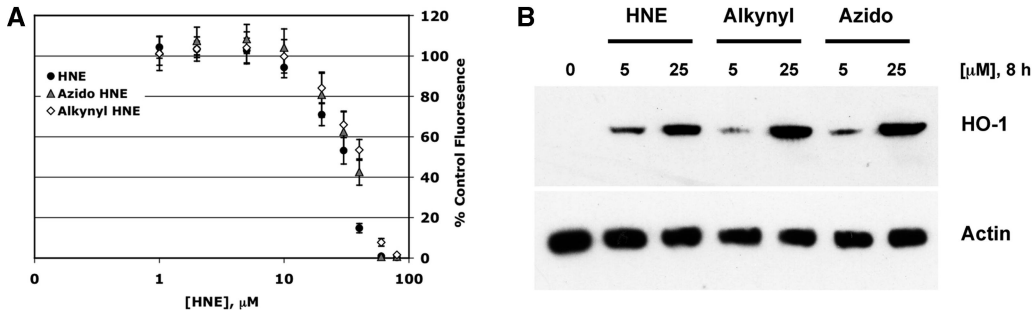

Figure 1. Comparison of HNE, Az-HNE, and Al-HNE towards cell toxicity and induction of heme-oxygenase-1 (HO-1) expression. Cell viability assays were done with cells seeded in 96-well plates at a density of 7.5×10^3 cells per well. After adhering overnight, cells were treated with HNE, Az-HNE, or Al-HNE (1–80 μM) in DMEM containing 10% fetal bovine serum. After 48 h, cell viability was determined using calcein-AM. Data in panel A are represented as mean % control fluorescence (mean ratio of arbitrary fluorescence units of treated samples to DMSO-treated samples $\times$ 100). The error bars represent standard deviations ($n = 8$). Panel B shows a Western blot analysis of HO-1 induction in RKO cells. Cells were treated with 5 and 25 μM HNE, Az-HNE, or Al-HNE for 8 h. Cell were then lysed, and Western blot analysis was done using an anti HO-1 antibody.

Scheme 3. Synthesis of Biotinylating Reagents

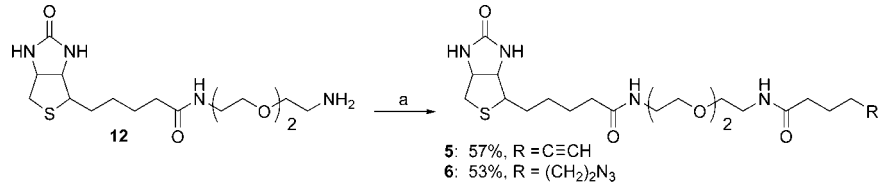

biotin tag contains an ethylene glycol linker to increase water solubility. Biotin was coupled to the linker to yield **12** as previously reported (*38*). Reaction of **12** with 5-hexynoyl chloride or 6-azidohexanoyl chloride produced the desired tags **5** and **6**, respectively.

Peptide Adduction with HNE and Analogues. The HNE analogues were designed to minimize structural variations compared to those of native HNE that may result in a change in reactivity. In order to compare the reactivity of **2** and **3** relative to **1**, the adduction to several peptides was studied. Three peptides were chosen that contained His, Lys, or Cys, major sites of HNE adduction: Angiotensin II (Asp-Arg-Val-Tyr-Ile-His-Pro-Phe), Thymic humoral gamma 2 factor (Leu-Glu-Asp-Gly Pro-Lys-Phe-Leu), and ANP (Ser-Leu-Arg-Arg-Ser-Ser-Cys-Phe-Gly Gly Arg). Each peptide (1 mM) was incubated in the presence of **1**, **2**, or **3** (5 mM) at 37 °C, typically for 1 h. The reaction mixture was subsequently reduced with $NaBH_4$, neutralized, and analyzed by LC-MS for adduct formation. In all cases, reduced Michael and Schiff base adducts were observed, as well as a minor amount of a mixture of both adducts (see Supporting Information, Figure S1).

These qualitative experiments indicated that modification of the HNE structure did not impact the formation of Schiff base and Michael adducts. However, we were also interested in the relative reactivity of analogues **2** and **3** compared to **1**. Each peptide (0.7 mM) was incubated in the presence of an equimolar mixture of **1**–**3** (5 mM each) as described above, and aliquots were taken every hour. The samples were subsequently analyzed by LC-MS, and the amount of each HNE adduct was measured. For the peptides containing His and Lys, there was no significant difference between the relative amounts of adducts formed with each of the HNE analogues compared to native HNE. However, when the peptide contained Cys, there was approximately 50% less adduct in the presence of Az-HNE (Figure S2). The reason for the less efficient reaction of the Cys-containing peptide with Az-HNE is unknown, but it may be from thiol reduction of the azide moiety.

To further explore the reactivity of the HNE analogues and more closely mimic biological conditions, adduction experiments

Scheme 4. Click Chemistry of Peptide Adduct with Biotin Tag

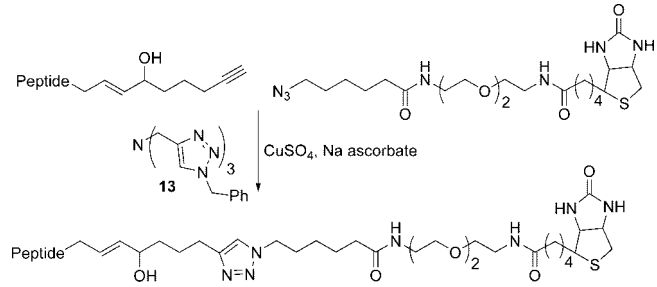

were carried out with an equimolar mixture of the peptides in the presence of each HNE compound. As expected, the Lys- and Cys-containing peptides were considerably more reactive than the His-containing peptide. Consistent with the previous experiment, analogues **2** and **3** exhibited reactivity similar to that of HNE, except when a Cys was present in the peptide. As observed in the HNE mixture experiments, incubation of Cys in the presence of Az-HNE generated approximately 50% less adduct (Figure S3).

Comparison of the Biological Activity of HNE and Analogues. The structural similarity of HNE to its analogues was also tested by comparing their relative toxicity and ability to induce heme-oxygenase-1 (HO-1) expression. RKO cells were treated with HNE, Az-, or Al-HNE, and cellular viability was determined after 48 h of incubation. As shown in Figure 1A, the cellular viability for HNE and its analogues are very similar. Induction of HO-1 expression with exposure of RKO cells to 25 μM HNE, Az-, or Al-HNE for 8 h was similar (Figure 1B). Therefore, Az- and Al-HNE are suitable analogues of HNE to probe the reactivity with proteins in vivo.

Click Chemistry Optimization of HNE-Adducted Peptides. Peptides adducted with either Al- or Az-HNE were subsequently tagged with biotin for affinity purification utilizing click chemistry (Scheme 4). The click reaction employs a Cu(I) catalyzed cyclization of an azide with an alkyne to form a stable triazole. There are a variety of reaction conditions published

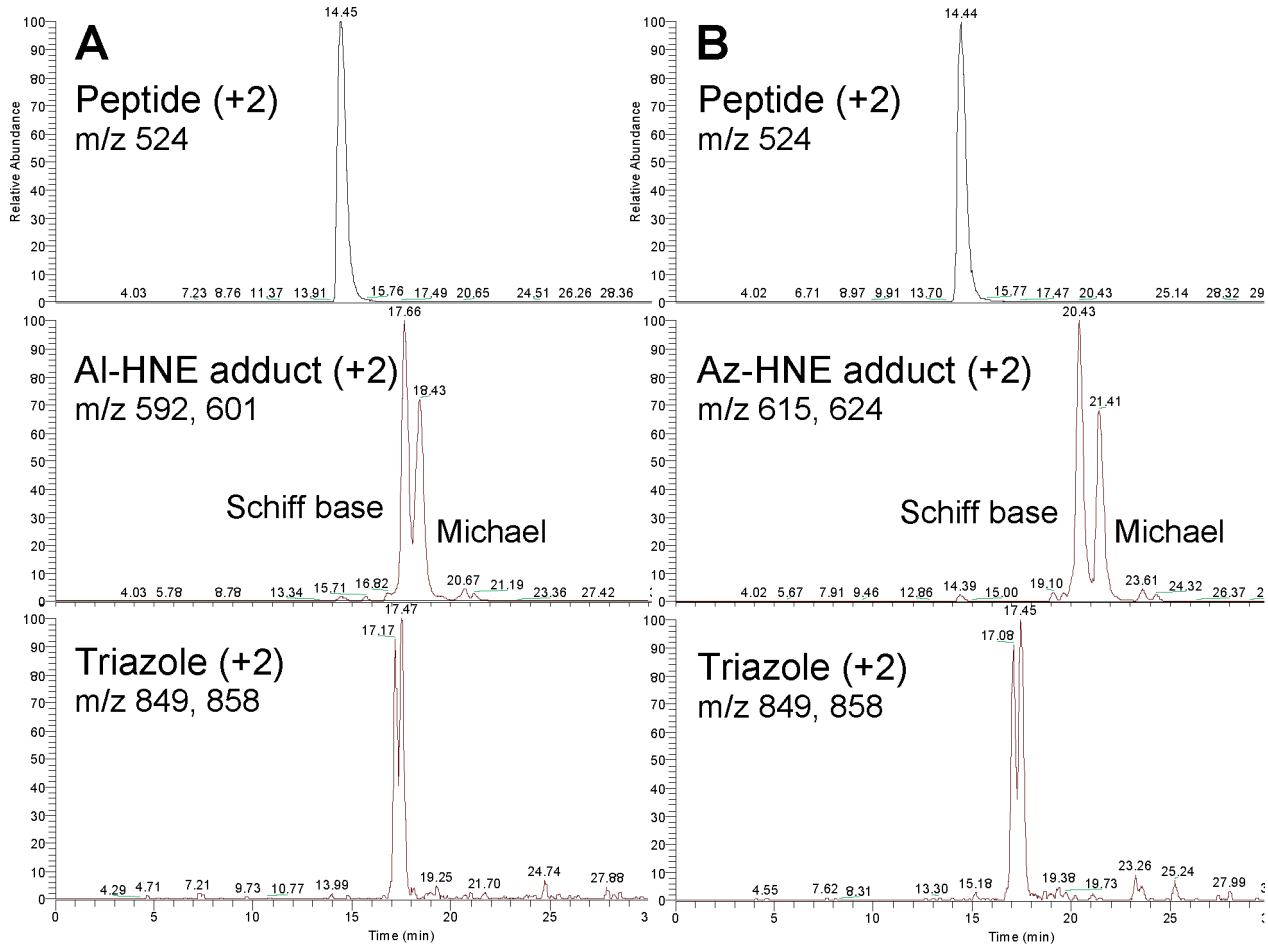

Figure 2. Incubation of Angiotensin with (A) Al-HNE and Az-biotin, and (B) Az-HNE and Al-biotin. From top to bottom are the unreacted peptide, peptide Schiff base and Michael adducts, and triazole. Angiotensin (1 mM) was incubated with Al- or Az-HNE (5 mM) at 37 °C for 1 h, then with Az- or Al-biotin (2–5 equiv), Asc (50 equiv), **13** (10 equiv), and $CuSO_4$ (50 equiv) for 1 h.

for this particular reaction; therefore, conditions were optimized for our particular reagents. The most striking differences are the $CuSO_4$ reducing agent and the choice of amine to stabilize the in situ formed Cu(I) species. We explored the use of tris(2-carboxyethyl)phosphine or Asc as the reducing agent, and ligand **13** or diisopropylethylamine (DIPEA) as the stabilizer. The peptide adduct was reacted with the appropriate biotin tag (**5** or **6**) under a variety of conditions, and the progress of the reaction was monitored by LC/MS.

From the studies on the click chemistry of the peptide adducts, we found that Asc was superior to TCEP as the $CuSO_4$ reducing agent. When TCEP was used, there was negligible triazole formation, as detected by LC/MS. Increasing the reaction time and equivalents of $CuSO_4$/TCEP had little effect on the reaction. In addition, the use of **13** or DIPEA did not increase the yield of triazole. However, when Asc was used as the reducing agent in conjunction with **13**, complete triazole formation was observed within 1 h. These latter reaction conditions were tested for all peptides mentioned above that had been adducted with either Al- or Az-HNE and subsequently reacted with Az- or Al-biotin, respectively. All adducted peptides were quantitatively converted to their biotin-tagged counterparts within 1 h. Shown in Figure 2 is a representative analysis of the peptide adduction and the subsequent click chemistry with the biotin tags to form triazole.

Biotin Labeling of Az-HNE-Adducted Protein in RKO Cells with the Staudinger Ligation. Initial studies were aimed at biotin labeling Az-HNE-adducted proteins using the modified Staudinger ligation. RKO cells labeled with Az-HNE were efficiently labeled with BiotTPhPh after 1 h of incubation (Figure 3). Cells exposed to 50, 100, and 150 μM Az-HNE were efficiently labeled with biotin as judged by the Western blot signal using HRP-SA, whereas there was no detectable biotin signal for cell samples treated with vehicle control.

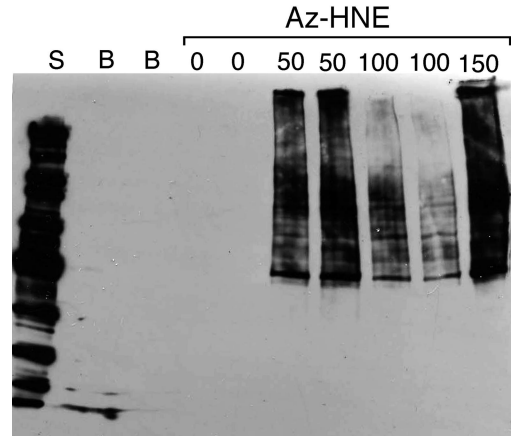

Figure 3. Staudinger ligation for biotin-labeling of Az-HNE adducted proteins in RKO cells. Intact RKO cells were incubated with Az-HNE (50, 100, and 150 μM) and vehicle control (DMSO) for 1 h. The cells were lysed as described in Materials and Methods and then incubated with 200 μM BiotTPhPh for 1 h. The degree of biotin labeling was determined by Western blotting using HRP-SA. Protein load was 2.5 μg per lane. S, biotin-labeled standards; B, RKO cells incubated with no DMSO; 0, RKO cells incubated with DMSO (1% v/v); 50, 100, and 150 are the concentrations of Az-HNE added to the cells in DMSO (1% v/v).

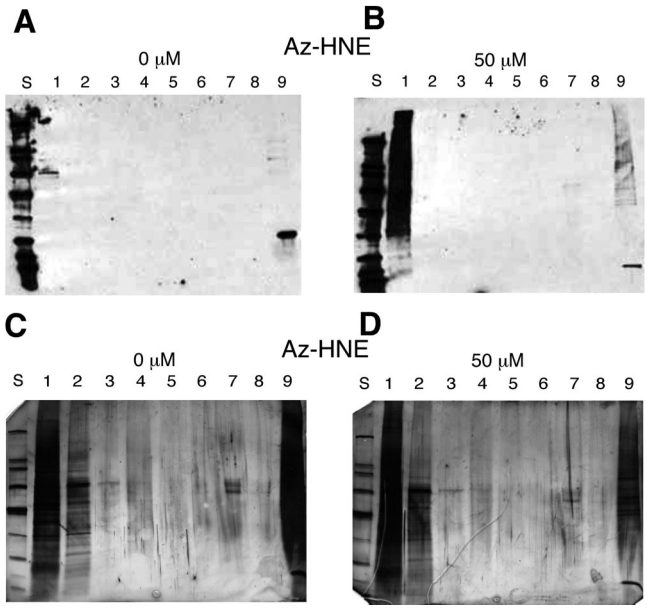

Figure 4. SA bead purification of biotin-tagged proteins produced from the Staudinger ligation. Cellular lysates (lane 1) containing biotin-tagged proteins (30 μL, ~7.5 μg of protein) were incubated with SA beads (30 μL; 1:1 in 0.1 M ammonium bicarbonate) for 1 h, then the beads and the breakthrough fraction (lane 2) were recovered by centrifugation. The beads were washed successively with ammonium bicarbonate (lane 3), 1 M NaCl with 1% Igepal (lane 4), ammonium bicarbonate (lane 5), and distilled H_2O (lane 6). Protein elution was done in two steps. lane 7 represents elution with 70% CH_3CN and 5% FA. lane 8 represents a wash with distilled H_2O, and lane 9 represents elution by boiling in laemmli buffer containing 5% β-mercaptoethanol. Panels A and C are the vehicle control samples, and panels B and D are 50 μM Az-HNE samples. Western blotting was performed in panels A and B, and silver stain analysis was done in panels C and D. S, biotin labeled standards.

Affinity Purification of Proteins Biotin-Tagged with the Modified Staudinger Ligation Using SA Beads. Purification of biotin-tagged proteins using SA beads was attempted prior to subsequent proteomic analysis. Western blot analysis demonstrated that biotin-tagged proteins readily bound to SA beads (lane 2, Figure 4B). Also, biotin-tagged proteins were retained on the SA beads in subsequent wash steps with significant elution of non-adducted proteins (lanes 3–6, Figure 4A and B). There was no elution of biotin-tagged proteins from SA beads using 70% CH_3CN and 5% FA (lane 7, Figure 4B); however, boiling the beads in laemmli buffer resulted in significant elution of biotin-tagged proteins (lane 9, Figure 4B). Unfortunately, detection of total proteins by silver stain analysis showed that there was significant contamination of nonadducted proteins with biotin-tagged proteins (compare lane 9 of Figure 4C and D). Therefore, biotin-tagged proteins from the modified Staudinger ligation were not affinity-purified with SA beads, and subsequent proteomic analysis was not performed.

Click Chemistry of Cellular Proteins Labeled with Az-HNE in RKO Cells. Click chemistry was applied to conjugate HNE-adducted proteins with biotin as an alternative to the Staudinger ligation. Intact RKO cells were treated with Az-HNE (1, 5, 10, 25, and 50 μM), then the time dependence of Al-Biot conjugation to Az-HNE adducted proteins from cellular lysates was tested using click chemistry. Lysates from cells treated with 50 and 25 μM Az-HNE reached maximal biotin labeling after 90 min of incubation as judged by HRP-SA detection by Western blotting (Figure 5D). Comparatively, lysates from cells treated with 5 and 10 μM Az-HNE needed 3–6 h of incubation for maximal labeling (Figure 5C). There was no detection of biotin-tagged proteins in DMSO control

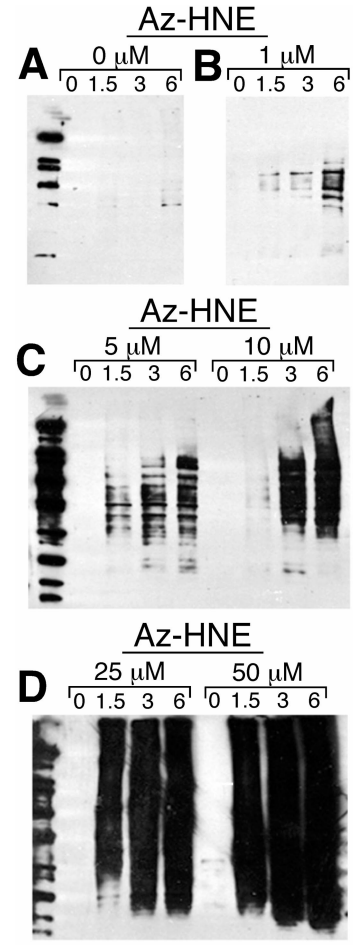

Figure 5. Time dependence of click chemistry for labeling Az-HNE adducted proteins in RKO cells. Intact RKO cells were incubated with Az-HNE (1, 5, 10, 25, and 50 μM) and vehicle control (DMSO) for 1 h. The cells were lysed as described in Materials and Methods and then incubated with biotin linker alkyne (600 μM), TCEP (6.0 mM), ligand (**13**, 0.75 mM), and $CuSO_4$ (6.0 mM) for 0, 1.5, 3, and 6 h. The degree of biotin labeling with click chemistry is determined by Western blotting using HRP-SA. Protein load was 2.5 μg/lane. The biotin labeling is shown for the control (panel A), 1 μM Az-HNE (panel B), 5 and 10 μM Az-HNE (panel C), and 25 and 50 μM (panel D).

samples up to 3 h of reaction (Figure 5A). However, there was a barely detectable signal in the DMSO controls after 6 h (Figure 5A). Biotin-tagged proteins from cells treated with as low as 1 μM Az-HNE were detected with a significantly higher signal compared to that of DMSO controls after 6 h of reaction (Figure 5B vs A, respectively). It is interesting to note that the click chemistry reaction occurred in cell lysates with TCEP as the reductant, whereas the same reaction did not occur with peptide adducts. This is puzzling; however, different reaction conditions (i.e., Az-HNE-adducted peptides in aqueous solution vs Az-HNE-adducted proteins in crude cell lysates) may have contributed to this difference. Click chemistry reactions performed with cell lysates in the presence of ascorbate were complete after ~5 min (data not shown), as compared to ~90 min for TCEP. The much higher rate for the click chemistry reaction with ascorbate compared to that for TCEP is consistent with the model peptide studies. However, biotin-tagged proteins were not affinity purified from nonmodified proteins with SA beads when ascorbate was used as the reductant (data not shown). As shown below, using TCEP as the reductant resulted in specific recovery of biotin-tagged proteins. Therefore, TCEP was used in further experiments.

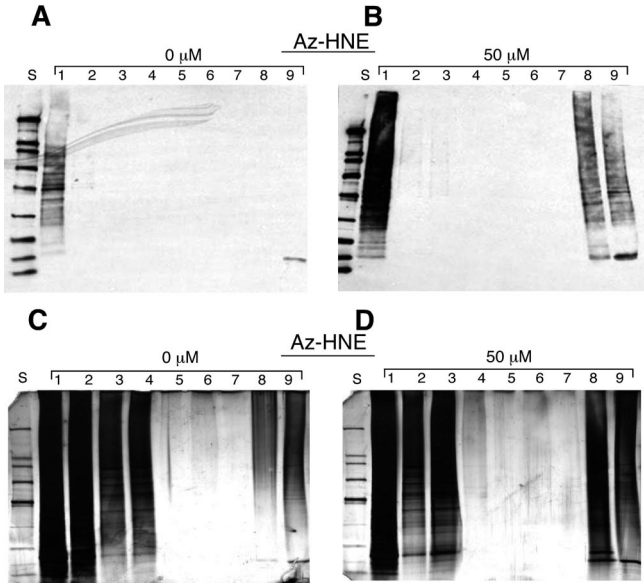

Figure 6. SA bead purification of Az-HNE adducted protein conjugated to biotin. Cellular lysates (lane 1) containing biotin-tagged proteins (~150 μg) were incubated with SA beads (75 μL; 1:1 in ammonium bicarbonate) overnight, and then the beads were recovered in the morning, and the breakthrough fraction (lane 2) was collected. The beads were washed successively with ammonium bicarbonate (lane 3), 2 times with 1 M NaCl with 1% Igepal (lane 4 and 5), ammonium bicarbonate (lane 6), and distilled H_2O (lane 7). Protein elution was done in two steps. Lane 8 represents elution with 70% CH_3CN and 5% FA, and lane 9 represents elution by boiling in laemmli buffer containing 5% β-mercaptoethanol. Panels A and C are the vehicle control samples, and panels B and D are the 50 μM Az-HNE samples. Western blotting was performed in panels A and B, and silver stain analysis was done in panels C and D. S, biotin-labeled standard curve.

Streptavidin Purification of Proteins Biotin-Tagged with Click Chemistry. Biotin-tagged proteins from lysates of cells treated with Az-HNE (5, 10, or 50 μM) were affinity purified with SA beads. Western blot analysis demonstrates that biotin-tagged proteins from lysates of cells treated with 50 μM Az-HNE were efficiently captured with SA beads (lane 2, Figure 6B) with no detectable proteins in the elution fractions (lanes 3–7, Figure 6B). Figure 6B shows the elution of biotin-tagged proteins using 70% CH_3CN and 5% FA (lane 8) and boiling in laemmli buffer (lane 9). As shown in Figure 6A, DMSO controls had a low biotin signal in cell lysates (lane 1), breakthrough (lane 2), wash (lanes 3–7), or elution (lanes 8–9) fractions. The same fractions analyzed by Western blotting were tested by silver stain analysis for total protein detection. The lysate and flow through lanes (lanes 1 and 2, Figure 6C and D) had similar levels of total protein for both the control and 50 μM Az-HNE treated samples, and the wash steps had higher levels of total protein in the sample for 50 μM Az-HNE-treated samples compared to that in control samples, respectively (lanes 3–5, Figure 6D and C, respectively). In the CH_3CN elution step, significantly more proteins were eluted from SA beads incubated with the 50 μM Az-HNE treated sample versus controls (lane 8, Figure 6D and C, respectively). Similar protein bands were observed in the eluant from boiling SA beads for both the control and 50 μM Az-HNE-treated samples (lane 9, Figure 6C and D, respectively). Therefore, biotin-tagged proteins were selectively enriched relative to nontagged proteins by elution from SA beads with 70% CH_3CN and 5% FA.

Proteomic Analysis of Proteins Isolated with SA Beads. The total number of proteins identified from cells treated with vehicle control, 5, 10, and 50 μM Az-HNE-treated samples were 32, 41, 107, and 118, respectively. Proteins unique to the 5, 10, and 50 μM Az-HNE-treated cells compared to vehicle controls were 12, 58, and 91, respectively. A complete list of unique protein targets from Az-HNE treatment is displayed in Supporting Information (Table S1). The number of proteins identified corresponded to the concentration of Az-HNE used (i.e., increase in protein hits with increasing Az-HNE concentration), suggesting that the method is specific for HNE adduction of proteins. There were 39 common proteins identified between 50 and 10 μM Az-HNE-treated samples (Table S1). Also, 8 out of 12 proteins identified in the 5 μM sample were also present in the 50 μM sample (Table S1). Overall, the unique proteins found in the 50 μM Az-HNE-treated samples had better quality MS/MS spectra, more distinct peptides identified, and greater sequence coverage compared to the 10 and 5 μM treated samples (data not shown). Table 1 shows a select list of stress signaling proteins corresponding to the heat shock response and ER stress response such as Hsp70 and Hsp90, 78-kDa glucose regulated protein (GRP-78), respectively, as well as proteins involved in redox regulation, xenobiotic metabolism, and protein folding (glutathione-*S*-transferase Pi, peroxiredoxin-1, and the 60 kDa mitochondrial heat shock protein, respectively). Hsp70, Hsp90, and protein disulfide isomerase isoform A3 (PDIA3) were identified previously as being modified by HNE in vivo (*15–17*). Table 2 shows the percent sequence coverage for the select list of proteins in correlation with the increase in Az-HNE concentration. GRP-78, peroxiredoxin-1, 60 kDa mitochondrial heat shock protein, and stress-70 protein are identified in the lowest Az-HNE concentration used (5 μM) and may represent significant targets of HNE adduction. Also, the percent sequence coverage for these proteins increases dramatically from 5 to 50 μM Az-HNE.

Click Chemistry and Proteomic Analysis of Biotin Conjugated to Al-HNE-Adducted Protein. To confirm the findings with Az-HNE, we repeated the same procedure with Al-HNE. In these experiments, we used 2 mg of cell lysates to obtain better MS/MS spectra and identification of proteins. We first used the same lysis buffer for Al-HNE-treated cells as with Az-HNE-treated cells. However, the conjugation of Az-Biot to Al-HNE-adducted proteins was negligible in the 5 and 10 μM Al-HNE-treated samples after several hours of click chemistry (data not shown). Therefore, we switched to using 100 mM HEPES at pH 7.5, 150 mM NaCl, 0.1 mM EDTA, and 1% Igepal as the lysis buffer. This resulted in efficient labeling of Al-HNE-adducted proteins with Az-Biot as shown in Figure 7 (lane 1; panel A for 0 and 5 μM, and panel B for 10 and 50 μM Al-HNE). There was an increase in biotin labeling of Al-HNE-adducted proteins from 5 to 50 μM Al-HNE as demonstrated with Az-HNE labeling (Figure 5). Affinity purification of biotin-tagged proteins from lysates of cells treated with 5, 10, and 50 μM Al-HNE is shown in Figure 7. There is efficient capture of biotin-tagged proteins with the 5 and 10 μM Al-HNE-treated sample (lanes 2–5, Figure 7A and B), with some flow through of biotin-tagged proteins in the 50 μM sample. Elution of biotin-tagged proteins from 5, 10, and 50 μM Al-HNE-treated samples is shown in lane 6 of Figures 7A and B.

Proteomic Analysis of Al-HNE Modified Proteins. The total numbers of proteins identified from the control, 5, 10, and 50 μM Al-HNE-treated RKO cells were 50, 276, 456, and 538. In comparison, 21, 171, 67, and 322 proteins were identified as adducted in the control, 5, 10, and 50 μM Az-HNE-treated cells, respectively, using 2 mg of cell lysate for click chemistry and SA bead purification. A complete list of proteins for Al-HNE and Az-HNE from 2 mg of cell lysates is shown in Supporting

Table 1. Select Proteins Identified by LC-MS/MS Analysis of Az-HNE Adducted Proteins[a]

protein	Swiss-Prot ID	function[b]	localization[c]
heat shock 70 kDa protein 1	P08107	protein folding	Cyt
heat shock 70 kDa protein 1L	P34931	protein folding	Cyt
heat shock 70 kDa protein 4	O14992	protein folding	Cyt
heat shock 90 kDa α−2	P07900	protein folding	Cyt
78 kDa glucose regulated protein	P11021	protein folding	ER
protein disulfide isomerase A3	P30101	protein folding	Cyt
glutathione-*S*-transferase-Pi	P09211	xenobiotic metabolism	Cyt
peroxiredoxin-1	Q06830	redox regulation	Cyt
60 kDa mitochondrial heat shock protein	P10809	protein trafficking, protein folding	MT
stress-70 protein	P38646	cell proliferation	MT

[a] Proteins are selected from experiments with intact RKO cells treated with 50 μM Az-HNE. Total protein content of the cell lysates was 150 μg prior to SA bead purification. [b] Protein function is taken from ingenuity analysis (http://www.ingeuity.com). [c] Protein localization is taken from the protein information resource Web site (http://pir.georgetown.edu). Cyt, cytoplasm; ER, endoplasmic reticulum; MT, mitochondria.

Table 2. Percent Coverage of Select Proteins Adducted by Az-HNE in RKO Cells[a]

protein	0 μM	5 μM	10 μM	50 μM
heat shock 70 kDa protein 1				9[b]
heat shock 70 kDa protein 1L				7
heat shock 70 kDa protein 4			6	8
heat shock 90 kDa α−2			3	6
78 kDa glucose regulated protein		9	23	24
protein disulfide isomerase A3				7
glutathione-*S*-transferase-Pi			23	36
peroxiredoxin-1		16	37	39
60 kDa mitochondrial heat shock protein		8	10	22
stress-70 protein		10	10	25

[a] This table represents the proteins identified from three different concentrations of Az-HNE applied exogenously to intact RKO cells. [b] The number value indicates the percent amino acid coverage of each protein identified by peptide fragmentation using LC-MS/MS analysis.

Table 3. Select Proteins Adducted by Both Al-HNE[a] and Az-HNE[b]

protein	0 μM	5 μM	10 μM	50 μM
heat shock 70 kDa protein 1	–[a], –[b]	17, 7	15, –	21, 12
heat shock 70 kDa protein 1L	–, –	9, 4	13, –	15, 9
heat shock 70 kDa protein 4	–, –	27, 9	33, 3	37, 18
heat shock 90 kDa α−2	–, 3	11, 4	14, 4	16, 6
78 kDa glucose regulated protein	13, 10	39, 27	34, 6	46, 33
protein disulfide isomerase A3	–, –	18, 23	19, 7	31, 26
glutathione-*S*-transferase-Pi	–, –	32, 18	48, 18	58, 5
peroxiredoxin-1	14, –	34, 11	28, 11	51, 13
60 kDa mitochondrial heat shock protein	9, 5	40, 23	44, 7	48, 47
stress-70 protein	12, 3	37, 23	42, 12	42, 30

[a] Percent coverage of select proteins from experiments using Al-HNE adducted proteins from RKO cells (2 mg of protein in cell lysates). [b] Percent coverage of proteins selected from Az-HNE adducted proteins in RKO cell lysates.

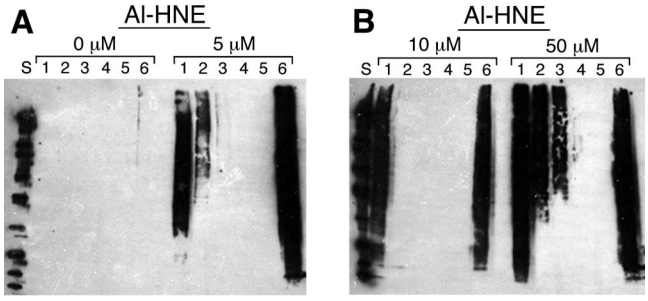

Figure 7. Streptavidin purification of Al-HNE adducted proteins conjugated with biotin. Cellular lysates (lane 1) containing Al-HNE adducted proteins conjugated with biotin (2 mg) were incubated with 1 mL of SA beads (1:1 in ammonium bicarbonate) for 2 h. After 2 h, the beads were recovered by centrifugation, and the breakthrough was collected (lane 2). Successive washes include 1% SDS (lane 3), 4 M urea (lane 4), and 1 M NaCl (lane 5). Elution of biotin-tagged proteins was done with 70% CH_3CN and 5% formic acid (lane 6). Biotin-tagged proteins were detected with HRP-SA, and 2.5 μg of protein was loaded per lane. Panel A shows the control (DMSO) and 5 μM Al-HNE, and panel B shows 10 and 50 μM Al-HNE. S, biotin-labeled standard curve.

Information (Tables S2 and S3). Table 3 shows that the same stress signaling and redox regulatory proteins were found from both Al- and Az-HNE treatment of RKO cells. We found that highly abundant proteins were identified in the DMSO control samples when 2 mg of cell lysate was used. Hsp90α-2 was found in control samples for Az-HNE-treated samples only, whereas GRP78, 60 kDa mitochondrial heat shock protein, and the stress-70 protein were identified in the control samples for Az-HNE- and Al-HNE-treated cells. Peroxiredoxin-1 was identified in control samples for Al-HNE-treated cells only. However, the percent coverage for these proteins increased dramatically over that of the control. This suggests that although these highly abundant proteins are identified in controls, they are specific for Al-HNE and Az-HNE modification. Furthermore, the percent coverage and overall similarity between the proteins identified using both Al-HNE or Az-HNE confirms that this method can reliably identify proteins adducted by HNE.

Discussion

This study reports the application of two different methods for labeling HNE-adducted proteins with biotin for subsequent enrichment and identification by proteomic analysis. The first method attempted to utilize the modified Staudinger ligation for the biotin conjugation of Az-HNE-adducted proteins. The Staudinger ligation selectively couples an azide with triphenylphosphine by reaction of a methyl ester ortho to triphenylphosphine, which captures the nucleophilic aza-ylide by intramolecular cyclization to form a stable amide bond and a phosphine oxide (Scheme 1) (*28*). Using BiotTPhPh, we specifically labeled Az-HNE-adducted proteins in lysates of RKO cells very efficiently with biotin (Figure 3). However, the results showed that biotin-conjugated proteins were not eluted from SA beads until their denaturation by boiling (lane 9, Figure 4B), which also resulted in the elution of nonspecific proteins (lane 9, Figure 4C and D). Attempts to remove the nonspecific proteins with very stringent washes, such as 5 M NaCl, 5% Igepal, or 4 M guanidine-HCl, failed (data not shown). It is unknown why the biotin-conjugated proteins did not elute in the 70% CH_3CN and 5% FA fraction, which was relatively free of nonlabeled proteins. The lack of affinity purification of these biotin-tagged proteins directed us to using click chemistry as an alternative to the modified Staudinger ligation for conjugating biotin to HNE-adducted proteins.

The copper-catalyzed Huisgen 1,3-dipolar cycloaddition reaction couples an azide with a terminal alkyne (*35*). Both azides and alkynes are stable in cells and in vivo, thus providing good probes for specifically labeling HNE modified proteins (*28, 31, 32, 43*). The reaction between the click chemistry reagents Az-HNE and Al-HNE with Al-Biot and Az-Biot, respectively, proceeded in the presence of TCEP in crude cell lysates, whereas in the peptide model studies, the reaction did not occur. Typically, the reactants and products from click chemistry reactions appear insoluble in aqueous buffer, yet the reaction proceeds more efficiently than in organic solvent (*34, 44*). A potential explanation for this, proposed by Kolb et al., is that organic molecules that are poorly soluble in aqueous solution have higher reaction kinetics because of a greater free energy than when soluble in organic solvents (*34*). We also observe insoluble particulates during click chemistry reactions in cellular lysates, thus potentially explaining the observed efficient biotin labeling in cell lysates compared to that in model peptide studies. However, the model studies clearly show that Asc is the better choice for a reductant for efficient click chemistry. Also, studies in cellular lysates demonstrate that Asc is a better reductant for click chemistry than TCEP. Others have used Asc as the reductant for click chemistry in model systems (*45*), but it has not been reported for biological systems. Biotin-tagged proteins from click chemistry reactions done in the presence of Asc were not affinity purified with SA beads. As judged by Coomassie staining, there was a similar profile of proteins that eluted from SA beads incubated with the DMSO control and 50 μM Az-HNE-treated samples. Metal-ion-catalyzed oxidation of proteins from the presence of oxidants generated from $CuSO_4$and Asc, such as hydroxyl radical or superoxide (*46*), may have resulted in enhanced binding with sepharose beads or caused the oligomerization of proteins. Oligomerization of proteins to biotin-tagged proteins would result in the appearance of nonspecific proteins following affinity purification steps. Therefore, TCEP was used for further experiments rather than ascorbate as the reductant for click chemistry.

Proteomic analysis of affinity-purified biotin-conjugated proteins showed that similar proteins were identified for Al- and Az-HNE treated RKO cells (Table 3). This is in accordance with other studies demonstrating that phenyl sulfonate ester probes modified with either an azide (PSN_3) or an alkyne (PS≡) used for activity-based protein profiling of serine esterases resulted in the identification of similar proteins (*31*). Also, the PSN_3 probe conjugation with the rhodamine−alkyne tag (Rh≡) occurred more readily than the PS≡ conjugation to the rhodamine−azide tag (RhN_3), but the latter reaction had fewer nonspecific interactions. Both reactions were reported to be complete within 1 h (*31*). By comparison, we observed a slower rate for click chemistry in RKO crude cell lysates with Az-HNE concentrations of 10 μM and lower (∼3–6 h). After 90 min, both 25 and 50 μM Az-HNE-treated samples were completely labeled, similar to the other study (*31*). In the present study, Al-HNE resulted in fewer nonspecific bands as judged by Western blot analysis in the control samples compared to that in Az-HNE-treated samples (lane 1, Figure 7A vs lane 1, Figure 6A). However, we observed more proteins in the Al-HNE-treated cells for the control, 5, 10, and 50 μM than for the Az-HNE-treated cells (50, 276, 456, and 538 vs 21, 171, 67, and 322). The percent coverage for the select proteins listed in Table 3 is similar between Al-HNE and Az-HNE sample sets. Both the Az- and Al-HNE probes are comparable in the proteins they modify and are similar in reactivity with peptides and toxicity in cells. One discrepancy between the in vitro and in vivo studies was the use of $NaCNBH_3$ following cell lysis to stabilize Az- and Al-HNE Schiff base adducts on Lys residues of proteins (*47*). However, reversible Michael adducts on Lys residues must be stabilized with $NaBH_4$ (*14*). Therefore, some Michael adducts to Lys may have been lost during workup procedures prior to proteomic analysis. Further studies will be aimed at characterizing HNE adducts on proteins using $NaBH_4$ to ensure the recovery of all adducts. Nonetheless, the method described in this study provides an unambiguous analysis of proteins modified by HNE in vivo.

This study identified several proteins that were identified as in vivo targets of activated derivatives of xenobiotics. Bromobenzene and mycophenolic acid adduct to protein disulfide isomerase isoform-A3 (PDIA3) in rat liver (*48, 49*). The small molecule, *S*-(1,1,2,2-tetrafluoroethyl)-L-cysteine (TFEC), was shown to adduct the 60 kDa mitochondrial heat shock protein and the stress-70 protein in rat kidney (*50*). Both halothane and bromobenzene were shown to adduct GRP-78 in rat liver (*49, 51*). Glutathione-*S*-transferase-Pi was adducted by acetaminophen and BHT in mouse liver (*52, 53*). Hsp-90α was adducted by BHT in mouse lung (*53*), and peroxiredoxin-1 was adducted by acetaminophen in mouse liver (*52*). HNE has been previously shown to adduct to Hsp70, Hsp90, and PDIA3 (*15–17*), all of which were also identified in this analysis.

A previous microarray experiment performed with RKO cells treated with HNE, over the same concentration range used in the present study, demonstrated that the expression of several stress signaling proteins was induced via the heat shock response and the ER stress response. Some of the proteins identified as targets of HNE in the present study play important roles in the control of these pathways. For example, several heat shock proteins (i.e., HSP-70, HSP-90, 60 kDa heat shock protein, mitochondrial precursor) and 78 kDa glucose-regulated protein precursor (GRP-78) (a regulator or ER stress), and stress-70 protein (mitochondrial protein involved in protein binding and cellular proliferation) were identified. GRP-78 and stress-70 protein were both strong hits with 8–11 unique peptides identified in lysates from cells treated with 50 μM Az-HNE (Table 1). Also, both proteins were identified at all Az-HNE concentrations used (50, 10, and 5 μM; Table 1). When using 2 mg of cellular lysate protein, several of the heat shock proteins and redox regulatory proteins were identified at concentrations as low as 5 μM Az- or Al-HNE. This method can be used for an unbiased analysis of HNE-modified proteins in cells and in vivo for attempting to understand the roles that protein modification plays in gene expression changes in response to oxidative stress.

Acknowledgment. This research was supported by funds from the National Institutes of Health (P01-ES013125). We are grateful to Simona Codreanu, Elizabeth Burnette, Hansen Wong, and Matt Szapacs for helpful discussions of proteomic analysis, and Andrew Felts for the synthesis of BiotTPhPh.

Supporting Information Available: Data comparing the adducts formed for HNE, Az-, and Al-HNE to Angiotension (Figure S1); data comparing the rates of adduct formation to three different peptides with an equimolar ratio of HNE:Az-HNE:Al-HNE (Figure S2); data comparing the ratio of adduct formation for HNE, Az-, and Al-HNE in the presence of an equimolar mixture of peptides (Figure S3); table showing all of the proteins identified from Az-HNE-adducted proteins affinity purified from cell lysates containing 150 μg of cellular protein (Table S1); and table showing all of the proteins identified in an experiment comparing Al- and Az-HNE-

adducted proteins from cell lysates containing 2 mg of cellular protein (Tables S2 and S3, respectively). This material is available free of charge via the Internet at http://pubs.acs.org.

References

(1) Marnett, L. J., Riggins, J. N., and West, J. D. (2003) Endogenous generation of reactive oxidants and electrophiles and their reactions with DNA and protein. *J. Clin. Invest. 111*, 583–593.

(2) Schneider, C., Tallman, K. A., Porter, N. A., and Brash, A. R. (2001) Two distinct pathways of formation of 4-hydroxynonenal. Mechanisms of nonenzymatic transformation of the 9- and 13-hydroperoxides of linoleic acid to 4-hydroxyalkenals. *J. Biol. Chem. 276*, 20831–20838.

(3) West, J. D., and Marnett, L. J. (2006) Endogenous reactive intermediates as modulators of cell signaling and cell death. *Chem. Res. Toxicol. 19*, 173–194.

(4) Uchida, K., Toyokuni, S., Nishikawa, K., Kawakishi, S., Oda, H., Hiai, H., and Stadtman, E. R. (1994) Michael addition-type 4-hydroxy-2-nonenal adducts in modified low-density lipoproteins: markers for atherosclerosis. *Biochemistry 33*, 12487–12494.

(5) Grune, T., Siems, W. G., Schonheit, K., and Blasig, I. E. (1993) Release of 4-hydroxynonenal, an aldehydic mediator of inflammation, during postischaemic reperfusion of the myocardium. *Int. J. Tissue React. 15*, 145–150.

(6) Sayre, L. M., Zelasko, D. A., Harris, P. L., Perry, G., Salomon, R. G., and Smith, M. A. (1997) 4-Hydroxynonenal-derived advanced lipid peroxidation end products are increased in Alzheimer's disease. *J. Neurochem. 68*, 2092–2097.

(7) Selley, M. L. (1998) (E)-4-hydroxy-2-nonenal may be involved in the pathogenesis of Parkinson's disease. *Free Radical Biol. Med. 25*, 169–174.

(8) Montine, T. J., Huang, D. Y., Valentine, W. M., Amarnath, V., Saunders, A., Weisgraber, K. H., Graham, D. G., and Strittmatter, W. J. (1996) Crosslinking of apolipoprotein E by products of lipid peroxidation. *J. Neuropathol. Exp. Neurol. 55*, 202–210.

(9) West, J. D., and Marnett, L. J. (2005) Alterations in gene expression induced by the lipid peroxidation product, 4-hydroxy-2-nonenal. *Chem. Res. Toxicol. 18*, 1642–1653.

(10) Ji, C., Kozak, K. R., and Marnett, L. J. (2001) IkappaB kinase, a molecular target for inhibition by 4-hydroxy-2-nonenal. *J. Biol. Chem. 276*, 18223–18228.

(11) Neely, M. D., Sidell, K. R., Graham, D. G., and Montine, T. J. (1999) The lipid peroxidation product 4-hydroxynonenal inhibits neurite outgrowth, disrupts neuronal microtubules, and modifies cellular tubulin. *J. Neurochem. 72*, 2323–2333.

(12) Dinkova-Kostova, A. T., Holtzclaw, W. D., Cole, R. N., Itoh, K., Wakabayashi, N., Katoh, Y., Yamamoto, M., and Talalay, P. (2002) Direct evidence that sulfhydryl groups of Keap1 are the sensors regulating induction of phase 2 enzymes that protect against carcinogens and oxidants. *Proc. Natl. Acad. Sci. U.S.A. 99*, 11908–11913.

(13) Levonen, A. L., Landar, A., Ramachandran, A., Ceaser, E. K., Dickinson, D. A., Zanoni, G., Morrow, J. D., and Darley-Usmar, V. M. (2004) Cellular mechanisms of redox cell signalling: role of cysteine modification in controlling antioxidant defences in response to electrophilic lipid oxidation products. *Biochem. J. 378*, 373–382.

(14) Sayre, L. M., Lin, D., Yuan, Q., Zhu, X., and Tang, X. (2006) Protein adducts generated from products of lipid oxidation: focus on HNE and one. *Drug Metab. Rev. 38*, 651–675.

(15) Carbone, D. L., Doorn, J. A., Kiebler, Z., Ickes, B. R., and Petersen, D. R. (2005) Modification of heat shock protein 90 by 4-hydroxynonenal in a rat model of chronic alcoholic liver disease. *J. Pharmacol. Exp. Ther. 315*, 8–15.

(16) Carbone, D. L., Doorn, J. A., Kiebler, Z., and Petersen, D. R. (2005) Cysteine modification by lipid peroxidation products inhibits protein disulfide isomerase. *Chem. Res. Toxicol. 18*, 1324–1331.

(17) Carbone, D. L., Doorn, J. A., Kiebler, Z., Sampey, B. P., and Petersen, D. R. (2004) Inhibition of Hsp72-mediated protein refolding by 4-hydroxy-2-nonenal. *Chem. Res. Toxicol. 17*, 1459–1467.

(18) Hartley, D. P., Kroll, D. J., and Petersen, D. R. (1997) Prooxidant-initiated lipid peroxidation in isolated rat hepatocytes: detection of 4-hydroxynonenal- and malondialdehyde-protein adducts. *Chem. Res. Toxicol. 10*, 895–905.

(19) Hartley, D. P., Kolaja, K. L., Reichard, J., and Petersen, D. R. (1999) 4-Hydroxynonenal and malondialdehyde hepatic protein adducts in rats treated with carbon tetrachloride: immunochemical detection and lobular localization. *Toxicol. Appl. Pharmacol. 161*, 23–33.

(20) Bennaars-Eiden, A., Higgins, L., Hertzel, A. V., Kapphahn, R. J., Ferrington, D. A., and Bernlohr, D. A. (2002) Covalent modification of epithelial fatty acid-binding protein by 4-hydroxynonenal in vitro and in vivo. Evidence for a role in antioxidant biology. *J. Biol. Chem. 277*, 50693–50702.

(21) Perluigi, M., Fai Poon, H., Hensley, K., Pierce, W. M., Klein, J. B., Calabrese, V., De Marco, C., and Butterfield, D. A. (2005) Proteomic analysis of 4-hydroxy-2-nonenal-modified proteins in G93A-SOD1 transgenic mice--a model of familial amyotrophic lateral sclerosis. *Free Radical Biol. Med. 38*, 960–968.

(22) Uchida, K., Itakura, K., Kawakishi, S., Hiai, H., Toyokuni, S., and Stadtman, E. R. (1995) Characterization of epitopes recognized by 4-hydroxy-2-nonenal specific antibodies. *Arch. Biochem. Biophys. 324*, 241–248.

(23) Uchida, K., Szweda, L. I., Chae, H. Z., and Stadtman, E. R. (1993) Immunochemical detection of 4-hydroxynonenal protein adducts in oxidized hepatocytes. *Proc. Natl. Acad. Sci. U.S.A. 90*, 8742–8746.

(24) Lin, D., Lee, H. G., Liu, Q., Perry, G., Smith, M. A., and Sayre, L. M. (2005) 4-Oxo-2-nonenal is both more neurotoxic and more protein reactive than 4-hydroxy-2-nonenal. *Chem. Res. Toxicol. 18*, 1219–1231.

(25) Soreghan, B. A., Yang, F., Thomas, S. N., Hsu, J., and Yang, A. J. (2003) High-throughput proteomic-based identification of oxidatively induced protein carbonylation in mouse brain. *Pharm. Res. 20*, 1713–1720.

(26) Grimsrud, P. A., Picklo, M. J. Sr., Griffin, T. J., and Bernlohr, D. A. (2007) Carbonylation of adipose proteins in obesity and insulin resistance: identification of adipocyte fatty acid-binding protein as a cellular target of 4-hydroxynonenal. *Mol. Cell Proteomics 6*, 624–637.

(27) Yan, L. J., Orr, W. C., and Sohal, R. S. (1998) Identification of oxidized proteins based on sodium dodecyl sulfate-polyacrylamide gel electrophoresis, immunochemical detection, isoelectric focusing, and microsequencing. *Anal. Biochem. 263*, 67–71.

(28) Saxon, E., and Bertozzi, C. R. (2000) Cell surface engineering by a modified Staudinger reaction. *Science 287*, 2007–2010.

(29) Hang, H. C., Yu, C., Kato, D. L., and Bertozzi, C. R. (2003) A metabolic labeling approach toward proteomic analysis of mucin-type O-linked glycosylation. *Proc. Natl. Acad. Sci. U.S.A. 100*, 14846–14851.

(30) Speers, A. E., and Cravatt, B. F. (2005) A tandem orthogonal proteolysis strategy for high-content chemical proteomics. *J. Am. Chem. Soc. 127*, 10018–10019.

(31) Speers, A. E., and Cravatt, B. F. (2004) Profiling enzyme activities in vivo using click chemistry methods. *Chem. Biol. 11*, 535–546.

(32) Wang, Q., Chan, T. R., Hilgraf, R., Fokin, V. V., Sharpless, K. B., and Finn, M. G. (2003) Bioconjugation by copper(I)-catalyzed azide-alkyne [3 + 2] cycloaddition. *J. Am. Chem. Soc. 125*, 3192–3193.

(33) Krasinski, A., Radic, Z., Manetsch, R., Raushel, J., Taylor, P., Sharpless, K. B., and Kolb, H. C. (2005) In situ selection of lead compounds by click chemistry: target-guided optimization of acetylcholinesterase inhibitors. *J. Am. Chem. Soc. 127*, 6686–6692.

(34) Kolb, H. C., Finn, M. G., and Sharpless, K. B. (2001) Click Chemistry: Diverse Chemical Function from a Few Good Reactions. *Angew. Chem., Int. Ed. 40*, 2004–2021.

(35) Kolb, H. C., and Sharpless, K. B. (2003) The growing impact of click chemistry on drug discovery. *Drug Discovery Today 8*, 1128–1137.

(36) Hopf, H., and Kruger, A. (2001) Synthesis of cyclo-1,3-dien-5-ynes. *Chemistry 7*, 4378–4385.

(37) Rodriguez Rivero, M., and Carretero, J. C. (2003) Intramolecular Pauson-Khand reactions of alpha,beta-unsaturated esters and related electron-deficient olefins. *J. Org. Chem. 68*, 2975–2978.

(38) Reizelman, A., Wigchert, S. C., del-Bianco, C., and Zwanenburg, B. (2003) Synthesis and bioactivity of labelled germination stimulants for the isolation and identification of the strigolactone receptor. *Org. Biomol. Chem. 1*, 950–959.

(39) Grandjean, C., Boutonnier, A., Guerreiro, C., Fournier, J. M., and Mulard, L. A. (2005) On the preparation of carbohydrate-protein conjugates using the traceless Staudinger ligation. *J. Org. Chem. 70*, 7123–7132.

(40) Pirali, T., Tron, G. C., and Zhu, J. (2006) One-pot synthesis of macrocycles by a tandem three-component reaction and intramolecular [3 + 2] cycloaddition. *Org. Lett. 8*, 4145–4148.

(41) Jentoft, N., and Dearborn, D. G. (1979) Labeling of proteins by reductive methylation using sodium cyanoborohydride. *J. Biol. Chem. 254*, 4359–4365.

(42) Dennehy, M. K., Richards, K. A., Wernke, G. R., Shyr, Y., and Liebler, D. C. (2006) Cytosolic and nuclear protein targets of thiol-reactive electrophiles. *Chem. Res. Toxicol. 19*, 20–29.

(43) Link, A. J., and Tirrell, D. A. (2003) Cell surface labeling of Escherichia coli via copper(I)-catalyzed [3 + 2] cycloaddition. *J. Am. Chem. Soc. 125*, 11164–11165.

(44) Speers, A. E., Adam, G. C., and Cravatt, B. F. (2003) Activity-based protein profiling in vivo using a copper(i)-catalyzed azide-alkyne [3 + 2] cycloaddition. *J. Am. Chem. Soc. 125*, 4686–4687.

(45) Glaser, M., and Arstad, E. (2007) "Click labeling" with 2-[18f]fluoroethylazide for positron emission tomography. *Bioconjugate Chem. 18*, 989–993.

(46) Buettner, G. R., and Jurkiewicz, B. A. (1996) Catalytic metals, ascorbate and free radicals: combinations to avoid. *Radiat. Res. 145*, 532–541.
(47) Isom, A. L., Barnes, S., Wilson, L., Kirk, M., Coward, L., and Darley-Usmar, V. (2004) Modification of cytochrome c by 4-hydroxy-2-nonenal: evidence for histidine, lysine, and arginine-aldehyde adducts. *J. Am. Soc. Mass Spectrom. 15*, 1136–1147.
(48) Shipkova, M., Beck, H., Voland, A., Armstrong, V. W., Grone, H. J., Oellerich, M., and Wieland, E. (2004) Identification of protein targets for mycophenolic acid acyl glucuronide in rat liver and colon tissue. *Proteomics 4*, 2728–2738.
(49) Koen, Y. M., and Hanzlik, R. P. (2002) Identification of seven proteins in the endoplasmic reticulum as targets for reactive metabolites of bromobenzene. *Chem. Res. Toxicol. 15*, 699–706.
(50) Bruschi, S. A., West, K. A., Crabb, J. W., Gupta, R. S., and Stevens, J. L. (1993) Mitochondrial HSP60 (P1 protein) and a HSP70-like protein (mortalin) are major targets for modification during S-(1,1,2,2-tetrafluoroethyl)-L-cysteine-induced nephrotoxicity. *J. Biol. Chem. 268*, 23157–23161.
(51) Witzmann, F. A., Jarnot, B. M., Parker, D. N., and Clack, J. W. (1994) Modification of hepatic immunoglobulin heavy chain binding protein (BiP/Grp78) following exposure to structurally diverse peroxisome proliferators. *Fundam. Appl. Toxicol. 23*, 1–8.
(52) Qiu, Y., Benet, L. Z., and Burlingame, A. L. (1998) Identification of the hepatic protein targets of reactive metabolites of acetaminophen in vivo in mice using two-dimensional gel electrophoresis and mass spectrometry. *J. Biol. Chem. 273*, 17940–17953.
(53) Meier, B. W., Gomez, J. D., Zhou, A., and Thompson, J. A. (2005) Immunochemical and proteomic analysis of covalent adducts formed by quinone methide tumor promoters in mouse lung epithelial cell lines. *Chem. Res. Toxicol. 18*, 1575–1585.

TX700347W